

11

The spin of the nucleon: polarized deep inelastic scattering

11.1 Introduction

The static or low energy properties of the ‘lighter’ baryons (the nucleons and the hyperons and their resonances) are quite well explained in the *constituent quark model*, in which a baryon is visualized as made up of three *constituent quarks* (up, down and strange) with masses typically of about one third of the nucleon mass (see, for example, Close, 1979). In this picture the properties of the baryons are calculated using a non-relativistic Schrödinger equation or some more sophisticated version thereof. But the essential point for our discussion is that an unexcited baryon corresponds to the ground state of the three-particle system in which all the quarks are in relative s-states with zero orbital angular momentum and with no explicit rôle being played by any gluonic degrees of freedom.

As a consequence the spin of the baryon is equal to the sum of the spins of its constituent quarks. For a baryon moving along the Z -axis with helicity $\Lambda = 1/2$ one would thus expect to have

$$\sum S_z^{\text{quarks}} = \frac{1}{2}, \quad (11.1.1)$$

where the sum is over the flavours of quark present in the baryon.

At the other end of the scale, for high energy interactions involving large momentum transfers, a baryon is visualized as made up of point-like constituents, *partons*, consisting of quarks and gluons. The partonic quarks have the same internal quantum numbers as the constituent quarks, but very different effective masses ($m_u \approx 4 \text{ MeV}/c^2$, $m_d \approx 7 \text{ MeV}/c^2$, $m_s \approx 125\text{--}150 \text{ MeV}/c^2$). The gluons are massless and mediate the strong force between the quarks. Originally this was a purely phenomenological picture but was later subsumed into the beautiful gauge theory of strong interactions, QCD (see, for example, Leader and Predazzi, 1996).

The precise relation between constituent quarks and partonic quarks is not known and, as we shall see, experiments on polarized deep inelastic scattering (DIS) raise intriguing questions as to how the spin of a baryon is related to the spins of its partonic quarks. In particular the analogue of (11.1.1) is now known to be significantly violated.

This experimental discovery of the European Muon Collaboration (EMC) at CERN in 1988 (Ashman *et al.*, 1988, 1989) came as a great surprise and catalysed a major programme of experimental investigation and a host of papers on the theoretical aspects of the problem, with some results as surprising as the experimental one had been.

Since high energy large-momentum-transfer interactions between baryons are determined by the QCD-controlled interaction of their constituents it is clearly of the greatest importance to know what the structure of a baryon is in term of its partonic quarks and gluons. This structure cannot be studied easily by theoretical methods since it involves the non-perturbative regime of a strong interaction field theory. Consequently one relies on information gleaned from experimental studies in which the hadron is probed by hard photons or W and Z bosons. The prime example is DIS, to which we now turn.

11.2 Deep inelastic scattering

Deep inelastic lepton–hadron scattering has played a seminal rôle in the development of our present understanding of the substructure of elementary particles. The discovery of Bjorken scaling in the late 1960s provided the critical impetus for the idea that elementary particles contain almost point-like constituents and for the subsequent invention of the parton model, in which the reaction (Fig. 11.1)

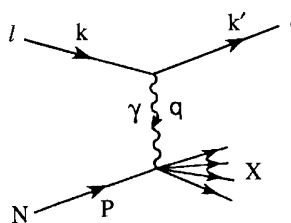


Fig. 11.1. Feynman diagram for inelastic lepton–nucleon scattering $lN \rightarrow lX$.

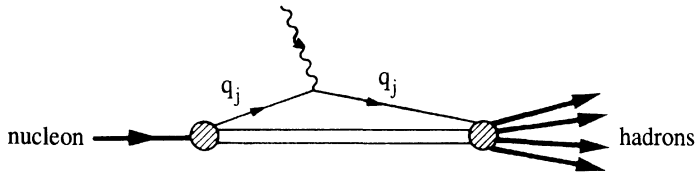


Fig. 11.2. Partonic interpretation of the lower part of the diagram in Fig. 11.1.

is viewed, as shown in Fig. 11.2, as the interaction of a hard virtual photon with a parton constituent of the nucleon. ('Hard' will mean $Q^2 \equiv -q^2 \gg M^2$, where M is the nucleon mass.)

DIS continued to play an essential rôle in the period of consolidation that followed, in the gradual linking of partons and quarks, in the discovery of the existence of missing constituents, later identified as gluons, and in the wonderful confluence of all the different parts of the picture into a coherent dynamical theory of quarks and gluons—quantum chromodynamics (QCD).

In more recent times the emphasis has shifted to the detailed study of the x -dependence of the parton distribution functions and to the study of their Q^2 -evolution, probably the most direct test of the perturbative aspects of QCD.

Polarized DIS, involving the collision of a longitudinally polarized lepton beam on a polarized target (either longitudinally or transversely polarized) provides a different, complimentary and equally important insight into the structure of the nucleon. Whereas ordinary DIS probes simply the number density of partons with a fraction x of the momentum of the parent hadron, polarized DIS can partly answer the more sophisticated question about the number density of partons with given x and given spin polarization, in a hadron of definite polarization.

But what is quite extraordinary and unexpected *ab initio* is the richness and subtlety of the dynamical effects associated with the polarized case. Whereas the unpolarized scaling functions $F_{1,2}(x)$ have a simple interpretation in the naive parton model (where the nucleon is considered as an ensemble of essentially free massless partons) and a straightforward generalization in the framework of perturbative QCD, the spin-dependent scaling functions $g_{1,2}(x)$ are much more subtle, each fascinating in its own way. The function $g_1(x)$, which, at first sight, seems trivial to deal with in the naive parton model, turns out to have an anomalous gluon contribution associated with it, within perturbative QCD. In addition the first moment of $g_1(x)$ turns out to be connected with an essentially non-perturbative aspect of QCD, the axial ghost that is invoked to resolve the

$U(1)$ problem of the mass of the η' . And $g_2(x)$ turns out not to have any interpretation at all in purely partonic language.

What is also fascinating is the extraordinary interplay of theory and experiment in the study of $g_1(x)$. For a long time the theory of $g_1(x)$ remained comfortably at the level of the naive parton model. Then, in 1988, came the disturbing result of the EMC, which differed significantly from the naive theoretical predictions. These results could be argued to imply that the expectation value of the sum of the spins carried by the quarks in a proton, $\langle S_z^{\text{quarks}} \rangle$, was consistent with zero rather than with $1/2$ as given in the quark model, suggesting a 'spin crisis in the parton model' (Leader and Anselmino, 1988). This led to an intense scrutiny of the basis of the theoretical calculation of $g_1(x)$ and the discovery of the anomalous gluon contribution (Efremov and Teryaev, 1988). (As often happens in theoretical physics it turns out that such an effect had already been studied to some extent in a largely overlooked paper of 1982 (Lam and Li, 1982).) So surprising was this discovery that the calculation was immediately checked by three different groups (Altarelli and Ross, 1988; Carlitz, Collins and Mueller, 1988; Anselmino and Leader, 1988), who all arrived at the same result. (Somewhat fortuitously, as it turns out, as was demonstrated in Carlitz *et al.*)

In the modified theoretical picture, the quantity $\Delta\Sigma \equiv 2\langle S_z^{\text{quark}} \rangle$, whose value had to be consistent with zero as a consequence of the EMC experiment, is replaced by the linear combination (for three flavours) $\Delta\Sigma - (3\alpha_s/2\pi)\Delta g$, where $\Delta g = \int_0^1 dx \Delta g(x)$ and $\Delta g(x)$ is the polarized gluon number density.

It has to be stressed that as a consequence of QCD a measurement of the first moment of $g_1(x)$ *does not* measure the z -component of the sum of the quark spins. It measures only the superposition $(1/9) [\Delta\Sigma - 3\alpha_s\Delta g/2\pi]$ and this linear combination can be made small by a cancellation between quark and gluon contributions. Thus the EMC results *cease to imply that $\Delta\Sigma$ is small*.

The function $g_2(x)$, however, does not have any simple interpretation in the naive parton model and it is a triumph of perturbative QCD that one can derive a sensible, gauge-invariant, result for it in the QCD field-theoretic model (Efremov and Teryaev, 1984).

In the following we shall concentrate almost exclusively on the polarized case. A good survey of the unpolarized case can be found in the review by Altarelli (1982) or, at a more introductory level, in Leader and Predazzi (1996).

For lack of space we shall also restrict our discussion almost entirely to *neutral current* interactions of the type (11.2.1), where the lepton is an electron or muon and the particle exchanged between the lepton and the hadron is a virtual photon. For very large Q^2 , Z^0 -exchange must also be

taken into account, but for the spin-dependent case of interest the present generation of experiments does not require that. Also of importance are the *charged current* reactions of the type.¹

$$l^- + N \rightarrow \nu_l + X, \quad (11.2.2)$$

which will be studied by the HERMES group at HERA. For a detailed discussion of these matters and the extension to nuclear targets, the reader should consult the review article of Anselmino, Efremov and Leader (1995).

Finally, a word about notation. In this chapter, in order to follow the convention in the literature, the covariant spin vector \mathcal{S}_μ (Section 3.4) for a spin-1/2 particle will be normalized in such a way that

$$\mathcal{S}^2 = -1. \quad (11.2.3)$$

Then for a fermion or antifermion of mass m and given \mathcal{S} one has from subsections 4.6.2 and 4.6.3 the following useful results:

$$\begin{aligned} \bar{u}(p, \mathcal{S})\gamma^\mu\gamma_5u(p, \mathcal{S}) &= -\bar{v}(p, \mathcal{S})\gamma^\mu\gamma_5v(p, \mathcal{S}) \\ &= 2m\mathcal{S}^\mu \end{aligned} \quad (11.2.4)$$

and for a massless fermion of helicity $\lambda = \pm 1/2$

$$\begin{aligned} \bar{u}(p, \lambda)\gamma^\mu\gamma_5u(p, \lambda) &= -\bar{v}(p, \lambda)\gamma^\mu\gamma_5v(p, \lambda) \\ &= 4\lambda p^\mu. \end{aligned} \quad (11.2.5)$$

11.3 General formalism and structure functions

Consider the reaction Fig. 11.1 in the Lab frame, where the proton is at rest. For the initial and final lepton momenta we write

$$k^\mu = (E, \mathbf{k}) \quad k'^\mu = (E', \mathbf{k}') \quad (11.3.1)$$

and for the initial nucleon momentum

$$P^\mu = (M, \mathbf{0}). \quad (11.3.2)$$

Then the differential cross-section to find the scattered lepton in solid angle $d\Omega$ with energy in the range $(E', E' + dE')$ can be written (see, for example, Leader and Predazzi, 1996)

$$\frac{d^2\sigma}{d\Omega dE'} = \frac{\alpha^2}{2Mq^4} \frac{E'}{E} L_{\mu\nu} W^{\mu\nu}, \quad (11.3.3)$$

¹ For spin-dependent measurements it has not been possible up to now to contemplate using a neutrino *beam*, because of the impossibility of polarizing the huge target needed. See, however, Section 11.10.

where $q = k - k'$ and α is the fine structure constant. In (11.3.3) the leptonic tensor $L_{\mu\nu}$ is given by QED as

$$L_{\mu\nu}(k, s; k', s') = [\bar{u}(k', s')\gamma_\mu u(k, s)]^* [\bar{u}(k', s')\gamma_\nu u(k, s)], \tag{11.3.4}$$

where s is the lepton covariant spin vector. It can be split into symmetric (S) and antisymmetric (A) parts under μ, ν interchange and, after summing over the spin of the final lepton, takes the form

$$L_{\mu\nu}(k, s; k') = 2 \left[L_{\mu\nu}^{(S)}(k; k') + iL_{\mu\nu}^{(A)}(k, s; k') \right] \tag{11.3.5}$$

where

$$L_{\mu\nu}^{(S)} = k_\mu k'_\nu + k'_\mu k_\nu - g_{\mu\nu}(k \cdot k' - m^2) \tag{11.3.6}$$

$$L_{\mu\nu}^{(A)}(k, s; k') = m\epsilon_{\mu\nu\alpha\beta} s^\alpha (k - k')^\beta. \tag{11.3.7}$$

The hadronic tensor $W_{\mu\nu}$, which contains the strong interaction dynamics, can be written in terms of four scalar *inelastic form factors*, $W_{1,2}$ and $G_{1,2}$, functions at most of q^2 and $P \cdot q$:

$$W_{\mu\nu}(q; P, \mathcal{S}) = W_{\mu\nu}^{(S)}(q; P) + iW_{\mu\nu}^{(A)}(q; P, \mathcal{S}) \tag{11.3.8}$$

with

$$\begin{aligned} \frac{1}{2M} W_{\mu\nu}^{(S)}(q; P) &= \left(-g_{\mu\nu} + \frac{q_\mu q_\nu}{q^2} \right) W_1(P \cdot q, q^2) \\ &+ \left[\left(P_\mu - \frac{P \cdot q}{q^2} q_\mu \right) \left(P_\nu - \frac{P \cdot q}{q^2} q_\nu \right) \right] \frac{W_2(P \cdot q, q^2)}{M^2} \end{aligned} \tag{11.3.9}$$

$$\begin{aligned} \frac{1}{2M} W_{\mu\nu}^{(A)}(q; P, \mathcal{S}) &= \epsilon_{\mu\nu\alpha\beta} q^\alpha \left\{ M\mathcal{S}^\beta G_1(P \cdot q, q^2) \right. \\ &\left. + \left[(P \cdot q)\mathcal{S}^\beta - (\mathcal{S} \cdot q)P^\beta \right] \frac{G_2(P \cdot q, q^2)}{M} \right\} \end{aligned} \tag{11.3.10}$$

Putting eqns (11.3.8) and (11.3.5) into (11.3.3) one finds

$$\frac{d^2\sigma}{d\Omega dE'} = \frac{\alpha^2}{Mq^4} \frac{E'}{E} \left[L_{\mu\nu}^{(S)} W^{\mu\nu(S)} - L_{\mu\nu}^{(A)} W^{\mu\nu(A)} \right]. \tag{11.3.11}$$

Note that only the antisymmetric part $W_{\mu\nu}^{(A)}$ depends on the nucleonic spin and that the cross-section (11.3.11) is independent of the nucleon spin if the lepton is unpolarized.

The spin-independent inelastic form factors $W_{1,2}$ and the spin-dependent ones $G_{1,2}$, which can be measured experimentally, are written in terms of

scaling functions $F_{1,2}$ and $g_{1,2}$ as follows:

$$MW_1(P \cdot q, Q^2) \equiv F_1 \quad \nu W_2(P \cdot q, Q^2) \equiv F_2 \quad (11.3.12)$$

$$\frac{(P \cdot q)^2}{\nu} G_1(P \cdot q, Q^2) \equiv g_1 \quad \nu(P \cdot q)G_2(P \cdot q, Q^2) \equiv g_2, \quad (11.3.13)$$

where ν is the energy of the virtual photon in the Lab,

$$\nu = E - E'. \quad (11.3.14)$$

The structure functions $F_{1,2}$ have played a seminal rôle in the history of elementary particle physics. They are, in principle, functions of the two variables, $P \cdot q$ and Q^2 or, equivalently, of Q^2 and ‘Bjorken- x ’ (we shall sometimes write x_{Bj} for clarity),

$$x \equiv \frac{Q^2}{2P \cdot q} = \frac{Q^2}{2M\nu}, \quad (11.3.15)$$

and were expected to decrease rapidly as Q^2 increases at fixed x as a consequence of the inability of an extended object – the proton – to absorb very large momentum transfers. The discovery of ‘Bjorken scaling’, i.e. that $F_{1,2}(Q^2, x)$ are almost independent of Q^2 in the *Bjorken limit* $Q^2 \rightarrow \infty$, x fixed, catalysed the invention of partons, hard point-like constituents within the proton, and led eventually to the invention of QCD.

The spin-dependent structure functions $g_{1,2}$ are much more difficult to measure, requiring polarized beams and targets, but, as mentioned in Section 11.2, tremendous progress has been made in the last decade, largely as a consequence of the stimulus provided by the remarkable results of the EMC collaboration at CERN.

The most direct way to measure $g_{1,2}$ is to utilize a longitudinally polarized beam and a nucleon target polarized either along the direction of the lepton beam or transversely to it and in the scattering plane. In each case one measures the cross-section difference upon reversal of the nucleon spin. Indicating lepton and nucleon spin directions by \rightarrow and \Rightarrow respectively, one has

$$\frac{d^2\sigma_{\rightarrow\Rightarrow}}{d\Omega dE'} - \frac{d^2\sigma_{\leftarrow\Leftarrow}}{d\Omega dE'} = -\frac{4\alpha^2 E'}{Q^2 E M \nu} [(E + E' \cos \theta)g_1 - 2xMg_2] \quad (11.3.16)$$

$$\frac{d^2\sigma_{\rightarrow\uparrow}}{d\Omega dE'} - \frac{d^2\sigma_{\rightarrow\downarrow}}{d\Omega dE'} = -\frac{8\alpha^2 (E')^2}{Q^2 M \nu^2} \left(\frac{\nu}{2E} g_1 + g_2 \right) \sin \theta \cos \phi \quad (11.3.17)$$

where θ is the Lab scattering angle of the lepton. Since θ is typically a few milliradians, it is much more difficult to make an accurate determination of the left-hand side of (11.3.17) than that of (11.3.16). The final-state-lepton azimuthal angle ϕ is defined in Fig. 11.18.

Because of the relative magnitudes of the coefficients of g_1 and g_2 in (11.3.16) and (11.3.17) it is usually assumed that the left-hand side of (11.3.16) is essentially a measurement of g_1 whereas the left-hand side of (11.3.17) largely determines g_2 . Only in the past year or so has it become possible to extract g_1 and g_2 from measurements of both these types of cross-section difference at the Stanford linear collider (see Abe *et al.*, 1997b, c; Anthony *et al.*, 1999).

In the following we shall first consider what is known theoretically about $g_{1,2}$ and then turn to consider the experimental situation. Note, incidentally, that (11.3.16) and (11.3.17) are not the only possible measurable quantities. For a more general approach, see Anselmino (1979).

11.4 The simple parton model

We shall sketch briefly how one derives parton-model expressions for $g_{1,2}$. For a very detailed and historical treatment see Leader and Predazzi (1996).

In an *infinite momentum frame* S^∞ , i.e. a Lorentz frame where the nucleon is moving very fast, the latter is visualized as made up of fast-moving constituents (partons) and the collision of the projectile with a constituent is treated in an impulse approximation, as if the constituent were a free particle.

If in this reference frame we imagine taking a snapshot of the target as seen by the projectile we may see a set of constituents of mass m_j and momenta p_j and we may ask for how long this fluctuation or virtual state will exist. Its lifetime, τ_V , by the uncertainty principle is likely to be of order $(\Delta E)^{-1}$,

$$\tau_V \simeq \frac{1}{\Delta E} = \frac{1}{E_V - E_N}, \quad (11.4.1)$$

where E_V is the energy of the virtual state and E_N the energy of the nucleon, in the given reference frame.

The impulse approximation will be valid when:

- (1) the time of interaction τ_{int} between the projectile and the constituent is much smaller than τ_V , so that the constituent is basically free during the period of its interaction with the projectile, and
- (2) the impulse given to the constituent is so large that after interaction its energy is much larger than the binding energy, and so it continues to behave as a free particle.

The second condition is automatically satisfied in the deep inelastic regime since a very large momentum is imported to the struck constituent. The first can be shown to be satisfied if the energy of internal motion of the

constituents is limited, say $O(M)$, where M is the mass of the nucleon, and one avoids events where x is very small.

In the impulse approximation the interaction of the projectile with the nucleon is simply an incoherent sum over its interactions with the individual constituents.

Let $n_q(\mathbf{p}, s; \mathcal{S}) d^3\mathbf{p}$ be the number of quark-partons q , charge e_q , with momentum in the range $\mathbf{p} \rightarrow \mathbf{p} + d\mathbf{p}$ and with covariant spin vector s^μ inside a nucleon of four-momentum P^μ with covariant spin vector \mathcal{S}^μ , as seen in the frame S^∞ .

Then one finds the rather intuitive result¹

$$W_{\mu\nu}^{(A)}(q; P, \mathcal{S}) = \sum_{q,s} e_q^2 \int d^3\mathbf{p} \left(\frac{P_0}{E_q} \right) \delta(2p \cdot q - Q^2) \times n_q(\mathbf{p}, s; \mathcal{S}) \tilde{w}_{\mu\nu}^{(A)}(q; p, s) \quad (11.4.2)$$

where $e_q^2 \tilde{w}_{\mu\nu} \delta(2p \cdot q - Q^2)$ is the analogue of $W_{\mu\nu}$ for the interaction of a hard photon with a ‘free’ quark-parton, as shown in Fig. 11.3. The factor P_0/E_q , where E_q is the energy of the struck quark, arises from the relativistic normalization of the states.

Since the parton in Fig. 11.3 is treated as an elementary, point-like charged fermion we can calculate $\tilde{w}_{\mu\nu}$ using QED, and the strong interaction dynamics is then hidden in the parton number-density or distribution functions in (11.4.2).

Note that since the whole approach only makes sense if the partons can be considered as essentially free, any result that turns out to depend critically on the parton mass must be treated with suspicion, because the mass of a constituent reflects its binding energy. Indeed, we shall see in a moment that for this very reason g_2 cannot be calculated reliably in the parton model (Anselmino, Efremov and Leader, 1995).

Now we consider the calculation of $\tilde{w}_{\mu\nu}^{(A)}$, describing as mentioned above the interaction of the hard photon with a quark of given flavour depicted in Fig. 11.3. The final state quark is a ‘free’ quark and is on the mass shell: $(p')^2 = m_q^2$. In the impulse approximation also the initial quark is

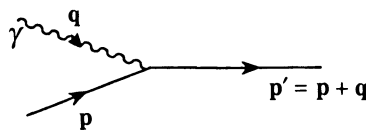


Fig. 11.3. Point-like interaction of a hard photon with a quark.

¹ An analogous result holds for the symmetric, spin-independent, part.

considered to be free and to have the same mass. But to see the potential danger of this assertion, let us put $p^2 = m^2$, where for the moment we allow $m^2 \neq m_q^2$ in order to represent the fact that the initial quark is really a bound quark. Aside from this we treat the incoming quark as free, i.e. its wave function is taken as the usual free-particle Dirac spinor $u(p, s)$ for a particle of mass m .

One then finds

$$\tilde{w}_{\mu\nu}(q; p, s) = \frac{1}{2} \text{Tr} [(1 + \gamma_5 \not{s})(\not{p} + m)\gamma_\mu(\not{p} + \not{q} + m_q)\gamma_\nu] \tag{11.4.3}$$

from which one obtains

$$\tilde{w}_{\mu\nu}^{(A)}(q; p, s) = (2\epsilon_{\mu\nu\alpha\beta})(m_q s^\alpha) \left[\left(1 - \frac{m}{m_q}\right) p^\beta - \frac{m}{m_q} q^\beta \right]. \tag{11.4.4}$$

Equation (11.4.4) is extremely revealing. We see immediately that for a general s^μ the result is not gauge invariant ($q^\mu \tilde{w}_{\mu\nu}^{(A)} \neq 0$) unless $m = m_q$. Moreover, the offending term, when $m \neq m_q$, is not small in an infinite-momentum frame (where the impulse approximation is supposed to be most justifiable) even if $m - m_q$ is small.

However, in the special case of longitudinal (L) polarization, if the quark has high momentum so that $m_q/p_z \ll 1$, the product $m_q s_L^\beta \rightarrow \pm p^\beta$ (see Section 3.4) and the non-gauge-invariant term vanishes because of the antisymmetric $\epsilon_{\mu\nu\alpha\beta}$ in (11.4.4). Let us therefore choose \mathcal{S}^β in (11.4.2) to correspond to a nucleon of definite helicity and s^α in (11.4.4) to correspond to a quark of definite helicity.

Then, putting (11.4.4) into (11.4.2) and integrating over the assumed-negligible quark transverse momentum, one finds, on comparing (11.4.2) and (11.3.10), that for a proton

$$g_1(x, Q^2) = \frac{1}{2} \sum_q e_q^2 [\Delta q(x) + \Delta \bar{q}(x)] \tag{11.4.5}$$

where

$$\Delta q(x) \equiv q_+(x) - q_-(x) \tag{11.4.6}$$

and q_\pm are the number densities of quarks with momentum fraction x and with helicity $\lambda = \pm 1/2$ respectively inside a *proton* of momentum P with helicity $\Lambda = +1/2$.

In terms of the original parton densities,

$$q_\lambda(x) \equiv P \int d^2 \mathbf{p}_\perp n_q(\mathbf{p}, \lambda; \Lambda = 1/2) \tag{11.4.7}$$

and the usual, unpolarized, number density is then

$$q(x) = q_+(x) + q_-(x). \tag{11.4.8}$$

Note that in (11.4.5) the sum is over all quarks and antiquarks. For antiquarks one commonly uses the notation $\Delta\bar{q}(x)$.

The result for g_1 seems to be unambiguous — it is not sensitive to the value of the quark mass. Yet, as we shall see later, (11.4.5) is not the full story because of the axial anomaly.

Quite the opposite happens for g_2 where the *transverse* spin is relevant. There is an extreme sensitivity to whether m equals m_q and one cannot expect to make a reliable calculation of $g_2(x)$ in the parton model.

One can put the case even more forcefully. The whole point of quarks is that, in their point-like interaction with a hard photon, they produce the large momentum-transfer reactions that we are trying to generate for the photon–hadron interactions. But even if we *define* the model by insisting that $m = m_q$, comparing the expression (11.4.4) with the general structure of $W_{\mu\nu}^{(A)}$ for a spin-1/2 particle (11.3.10), we see that

$$g_2(x)|_{\text{quark}} = 0. \quad (11.4.9)$$

Thus the hard-photon–free-quark interaction does not possess the cross-section asymmetry that we are seeking to explain in the photon–hadron interaction. It is clearly unrealistic therefore to try to produce such an asymmetry from quark-partons.

Of course the parton model predates QCD and, as treated above, is rather simplistic. Its value lies in the intuitive nature of its expressions in terms of parton number densities. When interactions come into play Bjorken scaling is broken and the main effect is that gluons become important and the parton densities get replaced by Q^2 -dependent densities $\Delta q(x, Q^2)$, whose Q^2 -dependence or evolution can be handled perturbatively.

We turn now to a more serious approach to the subject in the framework of field theory.

11.5 Field-theoretic generalization of the parton model

Historically there have been two approaches to DIS in QCD. The earlier one, the *operator product expansion* (OPE), concentrated on current commutators and their behaviour on the light-cone; the newer deals directly with Feynman diagrams. The latter is the more general and reproduces the OPE results wherever they are supposed to be valid. Neither is a complete scheme; in each, one has to make certain reasonable-sounding assumptions about the behaviour of non-calculable hadronic matrix elements of operators.

Because of its greater generality we shall base our treatment on the Feynman diagram field-theoretic approach.

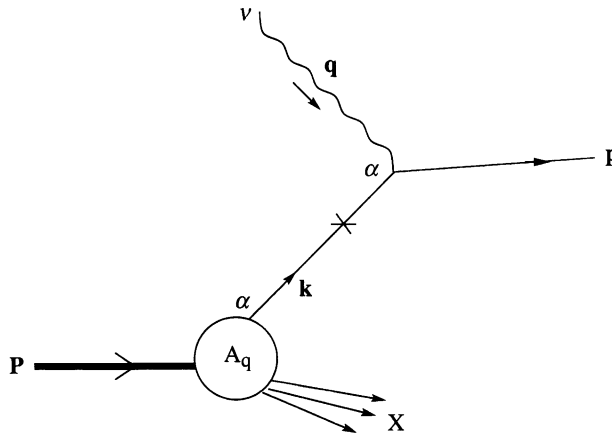


Fig. 11.4 Feynman diagram for $\gamma^* p \rightarrow \text{anything}$. The virtual photon has Lorentz index ν and momentum q ; the proton has momentum P .

The parton model, viewed as an impulse approximation, long predates QCD. Once QCD is accepted as a theory of the strong interactions it is clearly important to reformulate and extend the parton model using a field-theoretic framework.

We shall illustrate how this is carried out for the simplest case of deep inelastic scattering. For this purpose the rôle of the leptons is superfluous so we consider the reaction

$$\gamma^*(q) + p(P) \rightarrow \text{anything}$$

where the virtual photon has Lorentz index ν . The Feynman amplitude for this is shown in Fig. 11.4, where the amplitude has been split into a soft part controlling the emission of a quark from the proton and a hard part where the hard photon interacts with the quark. Note this is a *Feynman* diagram, not a probabilistic parton diagram. For simplicity we ignore flavour and colour; they may be dealt with trivially.

The soft vertex for the emission of a quark with Dirac spinor index α is called $A_{q\alpha}(k, X; P)$ and is defined to include the propagator for the quark of momentum k . The symbol \times on the quark line indicates that no propagator is to be inserted in the expression for the Feynman amplitude.

It will help to think of $A_q(k, X; P)$ as a column spinor. The Feynman amplitude is then

$$M^\nu(p, X; P) = \bar{u}_\lambda(p)(i\gamma^\nu)A_q(p - Q, X; P), \quad (11.5.1)$$

where, since it is inessential for our discussion, we have put the quark charge equal to unity.

A cross-section would involve the modulus squared of M^μ summed over all states X , and over the helicity λ of the final state quark and integrated over the momentum \mathbf{p} . However, because our virtual γ is actually attached to a lepton, we must sum over the Lorentz index ν . Hence we need to consider

$$w^{\mu\nu} \equiv \sum_\lambda \sum_X \int \frac{d^3\mathbf{p}}{2E(2\pi)^3} M^{\mu*} M^\nu (2\pi)^4 \delta^4(p + p_X - q - P). \tag{11.5.2}$$

Since M^μ is a number we can replace the complex conjugate by the hermitian conjugate \dagger , so that

$$\begin{aligned} w^{\mu\nu} &\equiv \sum_\lambda \sum_X \int \frac{d^3\mathbf{p}}{2E} A_q^\dagger (-i\gamma^{\mu\dagger}) \gamma^0 u_\lambda(p) \bar{u}_\lambda(p) (i\gamma^\nu) A_q \\ &\quad \times 2\pi \delta^4(p + p_X - q - P) \\ &= 2\pi \sum_X \int \frac{d^3\mathbf{p}}{2E} A_q^\dagger \gamma^0 (-i\gamma^\mu) \left\{ \sum_\lambda u_\lambda(p) \bar{u}_\lambda(p) \right\} (i\gamma^\nu) A_q \\ &\quad \times \delta^4(p + p_X - q - P) \end{aligned} \tag{11.5.3}$$

where we have used $\gamma^0 \gamma^{\mu\dagger} \gamma^0 = \gamma^\mu$. Carrying out the sum on λ , we can now write (11.5.2) in the form

$$w^{\mu\nu} = 2\pi \int \frac{d^3\mathbf{p}}{2E} \left\{ \sum_X \bar{A}_{q\beta} A_{q\alpha} \delta^4(p + p_X - q - P) \right\} \mathcal{E}^{\mu\nu}_{\beta\alpha} \tag{11.5.4}$$

where, obviously, $\bar{A}_q = A_q^\dagger \gamma^0$ and the hard, *short-distance*, piece is

$$\mathcal{E}^{\mu\nu}_{\beta\alpha} = [(-i\gamma^\mu)(\not{p} + m_q)(i\gamma^\nu)]_{\beta\alpha}. \tag{11.5.5}$$

The structure involving the soft vertices is written conventionally¹ as

$$\Phi_{\alpha\beta}(k = p - Q; P) = \sum_X \bar{A}_{q\beta} A_{q\alpha} \delta^4(p + p_X - q - P). \tag{11.5.6}$$

Note that the back-to-front convention for the Dirac indices α, β allows (11.5.6) to be written in matrix form

$$\begin{aligned} w^{\mu\nu} &= 2\pi \int \frac{d^3\mathbf{p}}{2E} \Phi_{\alpha\beta} \mathcal{E}^{\mu\nu}_{\beta\alpha} \\ &= 2\pi \int \frac{d^3\mathbf{p}}{2E} \text{Tr} (\Phi \mathcal{E}^{\mu\nu}) \end{aligned} \tag{11.5.7}$$

where Φ and $\mathcal{E}^{\mu\nu}$ are 4×4 matrices in Dirac spinor space.

¹ Sometimes in the literature Φ is defined with a factor $(2\pi)^4$ on the right-hand side of (11.5.6).

Finally we convert to $\int d^4p$ by using

$$\int \frac{d^3\mathbf{p}}{2E} = \int d^4p \delta(p^2 - m_q^2) \theta(E - m_q) \tag{11.5.8}$$

so that (11.5.7) can be written

$$w^{\mu\nu} = \int d^4p \text{Tr} (\Phi E^{\mu\nu}) \tag{11.5.9}$$

where, restoring the charge ee_f of the quark of flavour f ,

$$\begin{aligned} E^{\mu\nu} &= (ee_f)^2 2\pi \delta(p^2 - m_q^2) \theta(E - m_q) \mathcal{E}^{\mu\nu} \\ &= -(i\gamma^\mu ee_f) \left[(\not{p} + m_q) 2\pi \delta(p^2 - m_q^2) \theta(E - m_q) \right] (i\gamma^\nu ee_f). \end{aligned} \tag{11.5.10}$$

We shall now see that $E^{\mu\nu}$ is the discontinuity of the Feynman amplitude in Fig. 11.5, with external spinors and polarization vectors removed. For the latter amplitude has the form

$$M^{\mu\nu} = (i\gamma^\mu ee_f) \left[\frac{i(\not{p} + m_q)}{p^2 - m_q^2 + i\epsilon} \right] (i\gamma^\nu ee_f) \tag{11.5.11}$$

and using

$$\frac{1}{p^2 - m_q^2 + i\epsilon} = \text{P} \left(\frac{1}{p^2 - m_q^2} \right) - i\pi \delta(p^2 - m_q^2) \tag{11.5.12}$$

one will obtain a result for $E^{\mu\nu}$, if one makes the following replacement in the propagator in $M^{\mu\nu}$:

$$\begin{aligned} \frac{1}{p^2 - m_q^2 + i\epsilon} &\rightarrow \left(\frac{1}{p^2 - m_q^2 - i\epsilon} - \frac{1}{p^2 - m_q^2 + i\epsilon} \right) \theta(E - m_q) \\ &= 2i\pi \delta(p^2 - m_q^2) \theta(E - m_q). \end{aligned} \tag{11.5.13}$$

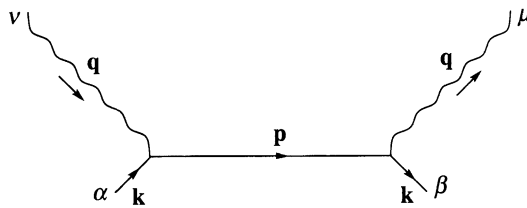


Fig. 11.5. Amputated Feynman diagram for $\gamma^*q \rightarrow \gamma^*q$. The virtual photon has Lorentz index ν and momentum q ; the quark has momentum k .

and $\Psi_\alpha(0)$ should be considered as column vectors in colour space. The combination in (11.5.6) is a colour singlet. Then

$$\begin{aligned}\Phi_{\alpha\beta} &= \sum_X \delta^4(p - p_X - q - P) \langle P | \bar{\Psi}_\beta(0) | X \rangle \langle X | \Psi_\alpha(0) | P \rangle \\ &= \sum_X \int \frac{d^4z}{(2\pi)^4} e^{ix \cdot (p + p_X - q - P)} \\ &\quad \times \langle P | \bar{\Psi}_\beta(0) | X \rangle \langle X | \Psi_\alpha(0) | P \rangle.\end{aligned}\quad (11.5.16)$$

Using translational invariance this becomes

$$\Phi_{\alpha\beta} = \int \frac{d^4z}{(2\pi)^4} e^{iz \cdot (p - q)} \sum_X \langle P | \bar{\Psi}_\beta(0) | X \rangle \langle X | \Psi_\alpha(z) | P \rangle$$

so that, using completeness, the sum over X can be carried out, yielding the final result

$$\Phi_{\alpha\beta}(P, \mathcal{S}, K) = \int \frac{d^4z}{(2\pi)^4} e^{ik \cdot z} \langle P, \mathcal{S} | \bar{\Psi}_\beta(0) \Psi_\alpha(z) | P, \mathcal{S} \rangle \quad (11.5.17)$$

where we have specified the proton state more precisely by including its covariant polarization vector \mathcal{S}^μ , and we have used $k = p - q$.

Thus Φ is expressed as a matrix element of a bilocal operator. It contains all the non-perturbative information about the state of a quark inside a proton in a given spin state. Φ is, at this stage, much more general than in the parton model, and if we expanded it in terms of a set of specific Dirac matrices, it would be hopeless to try to learn about the coefficient functions from experiment. To reach a manageable structure one has to make the key assumption that Φ decreases rapidly with increasing virtuality of the quark, i.e. as $|k^2|$ increases, and also decreases rapidly as $|P \cdot k|$ increases. These conditions guarantee that the dominant part of the k -integration region corresponds to the collinear situation $k^\mu \propto P^\mu$. We shall see later how these conditions are utilized to recover a structure recognizable as the parton model.

Φ is sometimes called the quark–quark correlation function. In reality it is the unnormalized density matrix of a virtual quark inside a proton. This can be seen by considering the expression for the cross-section of the process $\gamma^* + q(k) \rightarrow \gamma^* + q(k)$, with the initial virtual quark in an arbitrary state of polarization. One obtains the expression (11.5.14), of course without the d^4k integration, with Φ replaced by the density matrix of the initial quark.

The quark density matrix Φ was introduced in a seminal paper by Ralston and Soper (1979) and was generalized and much utilized by Efremov, Teryaev and collaborators (e.g. Efremov and Teryaev, 1984) and more recently by Mulders and collaborators (e.g. Mulders, 1997). The

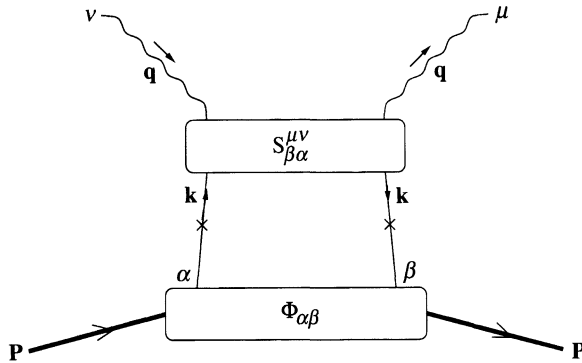


Fig. 11.8. Generalized version of Fig. 11.7.

most complete discussion of Φ and the analogous function for gluons can be found in the Ph.D. thesis of Boer (1998). See also Anselmino, Efremov and Leader (1995), Section 10 and Appendices B and C.

In the above discussion we used, for pedagogical purposes, the simplest possible diagram (Figs. 11.4 and 11.5) for the hard part of the scattering $\gamma^* + q \rightarrow q$. If one allows a more general perturbative QCD amplitude for the hard scattering, then the result (11.5.14) corresponding to Fig. 11.7 generalizes to

$$w^{\mu\nu} = \int d^4k \text{Tr} (\Phi S^{\mu\nu}) \tag{11.5.18}$$

corresponding to Fig. 11.8, in which $S_{\beta\alpha}^{\mu\nu}$ is the Feynman amplitude for $\gamma^{*\nu} + q \rightarrow \gamma^{*\mu} + q$, with external spinors and polarization vectors removed and with the replacement (11.5.13) made in the propagators.

We turn now to the question of reducing the general field-theoretic form (11.5.9) to the standard parton-model picture for polarized DIS.

Firstly, the hadronic tensor $W^{\mu\nu}$ is defined in such a way that for a quark of flavour f whose charge, in units of e is e_f ,

$$W^{\mu\nu} = \frac{1}{2\pi e^2} w^{\mu\nu} = \frac{1}{2\pi e^2} \int d^4k \text{Tr} (\Phi S^{\mu\nu}) \tag{11.5.19}$$

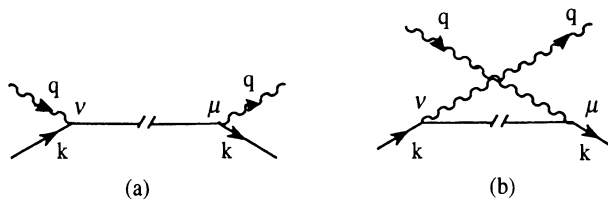


Fig. 11.9. Born diagrams for ‘hard’ γ^*q interaction.

The parton model usually emerges upon making the following approximations.

- (1) The γ^*q interaction is given its simplest form, as shown in Fig. 11.9. In the following we calculate only with the uncrossed Born diagram (a). The result for the crossed diagram is obtained at the end by the replacement $x_{Bj} \rightarrow -x_{Bj}$ in the hadronic matrix elements connected with $\Phi_{\alpha\beta}$ and is simply to be added to the uncrossed result. In order to isolate the antisymmetric part of $W^{\mu\nu}$ we make the replacements in (11.5.10)

$$\gamma^v \gamma^\rho \gamma^\mu \rightarrow \frac{1}{2} (\gamma^v \gamma^\rho \gamma^\mu - \gamma^\mu \gamma^\rho \gamma^v) = -i\epsilon^{\mu\nu\rho\sigma} \gamma_\sigma \gamma_5 \tag{11.5.20}$$

$$\gamma^v \gamma^\mu \rightarrow \frac{1}{2} (\gamma^v \gamma^\mu - \gamma^\mu \gamma^v) = i\sigma^{\mu\nu} \tag{11.5.21}$$

and recalling (11.3.8) we find

$$W_{\mu\nu}^{(A)} = \frac{e_f^2}{2} \int d^4k \delta \left[(k+q)^2 - m_q^2 \right] \left[\epsilon_{\mu\nu\rho\sigma} (q^\rho + k^\rho) \text{Tr} (\gamma^\sigma \gamma_5 \Phi) - m_q \text{Tr} (\sigma_{\mu\nu} \Phi) \right]. \tag{11.5.22}$$

- (2) One assumes that the soft matrix element cuts off rapidly for k^2 off the mass shell $k^2 = m_q^2$, and for k^μ non-collinear with respect to the hadron momentum P^μ . This is implemented as follows. Consider a reference frame where the hadron is moving at high momentum along OZ , so that

$$P^\mu = (E, 0, 0, P) \quad \text{with} \quad E \approx P \tag{11.5.23}$$

is a ‘large’ 4-vector. We introduce a ‘small’ null vector

$$n^\mu = \left(\frac{1}{P+E}, 0, 0, -\frac{1}{P+E} \right) \tag{11.5.24}$$

such that

$$n \cdot P = 1 \quad n^2 = 0. \tag{11.5.25}$$

One can then write for k^μ

$$k^\mu = (k \cdot n)P^\mu + \frac{1}{2} \left[\frac{k^2 + \mathbf{k}_T^2}{(k \cdot n)} - M^2(k \cdot n) \right] n^\mu + k_T^\mu \tag{11.5.26}$$

where

$$k_T^\mu = (0, \mathbf{k}_T, 0). \tag{11.5.27}$$

In view of the assumption about Φ we can say that

$$k^\mu \approx (k \cdot n)P^\mu. \tag{11.5.28}$$

It should be noted that some care is necessary in deciding whether the approximation (11.5.28) is adequate. We shall see that this depends crucially upon whether we are considering a nucleon with longitudinal (L) or with transverse (T) polarization.

11.5.1 Longitudinal polarization: the quark contribution to $g_1(x)$

For the study of g_1 we consider a nucleon with helicity $\lambda = \pm 1/2$ and it is sufficient to approximate (11.5.22) by putting

$$(q + k)^\rho \approx q^\rho + (k \cdot n)P^\rho \tag{11.5.29}$$

and dropping the term proportional to the quark mass m_q . Then writing

$$q^\rho + (k \cdot n)P^\rho = \int dx \delta(x - k \cdot n)(q + xP)^\rho \tag{11.5.30}$$

we can take the integration over d^4k in (11.5.22) through to obtain the antisymmetric component

$$W_{\mu\nu}^{(A)} = \frac{e_f^2}{2} \epsilon_{\mu\nu\rho\sigma} \int dx \frac{\delta(x - x_{Bj})}{2P \cdot q} (q + xP)^\rho A^\sigma(x), \tag{11.5.31}$$

where (using \mathcal{S}_L to denote longitudinal spin)

$$\begin{aligned} A^\sigma(x) &\equiv \int \frac{d^4k}{(2\pi)^4} d^4z \delta(x - k \cdot n) e^{ik \cdot z} \langle P, \mathcal{S}_L | \bar{\psi}(0) \gamma^\sigma \gamma_5 \psi(z) | P, \mathcal{S}_L \rangle \\ &= \int \frac{d\lambda}{2\pi} e^{i\lambda x} \langle P, \mathcal{S}_L | \bar{\psi}(0) \gamma^\sigma \gamma_5 \psi(\lambda n) | P, \mathcal{S}_L \rangle \end{aligned} \tag{11.5.32}$$

is a pseudovector which can depend only upon the vectors P^μ , n^μ and $v^\mu \equiv \epsilon^{\mu\alpha\beta\gamma} \mathcal{S}_\alpha P_\beta n_\gamma$ and the pseudovector \mathcal{S}^μ and which must be linear in \mathcal{S}^μ . Given that $\mathcal{S} \cdot P = 0$ the only possibilities are \mathcal{S}^σ and $(n \cdot \mathcal{S})P^\sigma$. Note that with the normalization

$$\langle \mathbf{P} | \mathbf{P}' \rangle = (2\pi)^3 2E \delta^3(\mathbf{P} - \mathbf{P}') \tag{11.5.33}$$

$A^\sigma(x)$ has dimensions $[M]$.

Recall that for a nucleon with 4-momentum given by (11.5.23)

$$\mathcal{S}^\mu(\lambda) = \frac{2\lambda}{M} (P, 0, 0, E) \quad \mathcal{S}^2 = -1, \tag{11.5.34}$$

where λ is the helicity ($\lambda = \pm 1/2$), so that

$$\mathcal{S}^\mu(\lambda) = \frac{2\lambda}{M} (P^\mu - M^2 n^\mu) \tag{11.5.35}$$

and we may take

$$\mathcal{S}^\mu(\lambda) \approx \frac{2\lambda}{M} P^\mu, \tag{11.5.36}$$

i.e. $M\mathcal{S}^\mu(\lambda)$ is a ‘large’ vector. In view of (11.5.36) the structures $(n \cdot \mathcal{S})P^\sigma$ and $\mathcal{S}^\sigma(\lambda)$ are equivalent in leading order and the only possibility is then (the factor 4 is for later convenience)

$$A^\sigma(x, \lambda) = 4Mh_L(x)\mathcal{S}^\sigma(\lambda) \tag{11.5.37}$$

where the dimensionless *longitudinal distribution function* is given by

$$4h_L(x) = \frac{n_\sigma A^\sigma(x)}{2\lambda} = \int \frac{d\tau}{2\pi} e^{i\tau x} \tilde{h}_L(\tau). \tag{11.5.38}$$

Here

$$\tilde{h}_L(\tau) = \frac{1}{Mn \cdot \mathcal{S}_L} \langle P, \mathcal{S}_L | \bar{\psi}(0) \not{n} \gamma_5 \psi(\tau n) | P, \mathcal{S}_L \rangle. \tag{11.5.39}$$

Substituting into (11.5.31) and adding the contribution from the crossed Born diagram, Fig. 11.9(b), yields

$$W_{\mu\nu}^{(A)}(L) = e_f^2 \frac{M}{P \cdot q} [h_L(x_{Bj}) + h_L(-x_{Bj})] \epsilon_{\mu\nu\rho\sigma} q^\rho \mathcal{S}^\sigma(\lambda). \tag{11.5.40}$$

Note that the term xP^ρ in (11.5.31) does not contribute on account of (11.5.36). Consequently (11.5.40) is gauge invariant, $q^\mu W_{\mu\nu}^{(A)} = 0$. Note that (11.5.36), which holds only for longitudinal spin, is crucial for the gauge invariance.

Comparing with (11.3.10) in the approximation $\mathcal{S}^\mu \propto P^\mu$ we obtain, for the contribution of a quark of flavour f ,

$$g_1(x) = \frac{1}{2} e_f^2 [h_L^f(x) + h_L^f(-x)]. \tag{11.5.41}$$

If one treats the quark fields in (11.5.39) as free fields and regards the nucleon as an assemblage of free partons one finds

$$h_L^f(x) = \Delta q_f(x) \qquad h_L^f(-x) = \Delta \bar{q}_f(x) \tag{11.5.42}$$

so that (11.5.41) reproduces the simple parton-model result for $g_1(x)$ in (11.4.5). Equation (11.5.41) provides a field-theoretic generalization of the parton-model result.

In the above we have been a little careless in not mentioning that most of the operators that appear require to be renormalized. That involves choosing a renormalization scale μ , and the matrix elements of the operators then depend upon μ . Physical, measurable quantities, of course, must not depend upon μ .

Although we shall be interested mainly in g_1 , it is instructive to compare the case above with the case of transverse polarization, which involves g_2 .

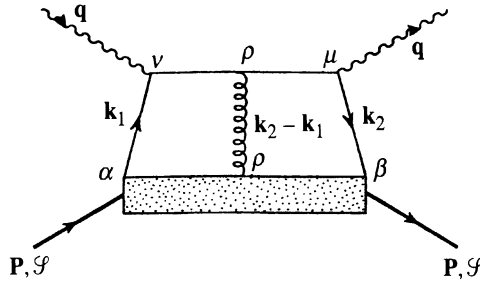


Fig. 11.10 Contribution to $\gamma^*p \rightarrow \gamma^*p$ involving quark–quark–gluon correlations.

11.5.2 Transverse polarization: $g_2(x)$

In order to see the essential difference between the longitudinal and transverse spin case, firstly consider again the result (11.5.40). In the CM of the γ^* –nucleon collision, for the longitudinal case we have, as far as magnitudes are concerned,

$$|q_\sigma| \sim |M \mathcal{S}_\sigma(\lambda)| = O(v) \quad P \cdot q = Mv \quad (11.5.43)$$

so that for the large components of $W_{\mu\nu}^{(A)}(L)$,

$$|W_{12}^{(A)}(L)| = O(v/M) \quad (11.5.44)$$

assuming that $|h_L(x)| = O(1)$. In the transverse spin case the analogue of (11.5.32) can only be proportional to \mathcal{S}_T^σ , since $n \cdot \mathcal{S}_T = 0$, and will produce a result like (11.5.40) with $\mathcal{S}(\lambda) \rightarrow \mathcal{S}_T$. Given that $|\mathcal{S}_T| = O(1)$ one has, for the ‘large’ components, only

$$|W_{\mu\nu}^{(A)}(L)| = O(1). \quad (11.5.45)$$

This immediately suggests that care must be exercised in neglecting non-leading terms, e.g. in (11.5.26).

Secondly, note that in (11.5.29) the term $(k \cdot n)P^\mu$ of (11.5.26) did not contribute because of the fact that, in leading order, $P^\mu \propto \mathcal{S}^\mu(\lambda)$. In the transverse case this will not happen and the analogue of (11.5.40) will contain a term $\epsilon_{\mu\nu\rho\sigma} P^\sigma \mathcal{S}_T^\sigma$ in $W_{\mu\nu}^{(A)}(T)$, which (analogously to the parton model case (11.4.4) when $m \neq m_q$) is not gauge invariant.

We must therefore return to (11.5.10) and improve upon approximation (11.5.28). However, it will then turn out that a more complicated, non-parton-model, diagram involving gluon exchange, Fig. 11.10, contributes to the same order.

Amazingly, as was shown by Efremov and Terayev (1984) this diagram just cancels the unwanted contribution from the $(k \cdot n)P$ and mass terms of the handbag diagram and the final result is gauge invariant. Essential in this proof is the use of the equations of motion for the quark field.

The analysis to show the cancellation is rather complicated and is carried out, for example, in Appendix C of Anselmino, Efremov and Leader (1995). It is helpful in this to utilize a definite QCD gauge $A_\mu^a(x) \cdot n^\mu = 0$, where $A_\mu^a(x)$ is the gluon vector potential of colour a . We shall only state the result here. It is the exact analogue of (11.5.40), namely, including the contribution of the crossed Born diagram in Fig. 11.9:

$$W_{\mu\nu}^{(A)}(T) = e_f^2 \frac{M}{P \cdot q} [f_T(x_{Bj}) + f_T(-x_{Bj})] \epsilon_{\mu\nu\rho\sigma} q^\rho \mathcal{S}_T^\sigma \tag{11.5.46}$$

where the analogue of (11.5.37) is

$$A^\sigma(x, T) = 4M f_T(x) \mathcal{S}_T^\sigma \tag{11.5.47}$$

with

$$4f_T(x) = \int \frac{d\tau}{2\pi} e^{i\tau x} \tilde{f}_T(\tau). \tag{11.5.48}$$

Here

$$\tilde{f}_T(\tau) = \frac{1}{M} \langle P, \mathcal{S}_T | \bar{\psi}(0) \gamma_5 \mathcal{S}_T \psi(\tau n) | P, \mathcal{S}_T \rangle. \tag{11.5.49}$$

Comparing (11.5.46) with (11.3.10), for the case of transverse polarization we obtain for the contribution of a quark of flavour f ,

$$g_1(x) + g_2(x) = \frac{e_f^2}{2} [f_T^f(x) + f_T^f(-x)]. \tag{11.5.50}$$

Although the surviving contribution comes from the ‘handbag’ diagram, it does not, in fact, have any simple parton interpretation. This looks mysterious given that (11.5.49) only involves *quark* fields. The subtle point is that (11.5.49) vanishes if the fields are treated as free fields and the nucleon as an assemblage of parallel moving quarks.

It is possible to obtain a non-zero result for $g_1(x) + g_2(x)$ if the partons are allowed to have transverse momentum \mathbf{k}_T , but the result then depends upon the specific assumption about the \mathbf{k}_T behaviour and is outside the traditional parton-model form.

11.6 Moments of the structure functions, sum rules and the spin crisis

Because of their relationship to the absorptive part of the scattering amplitudes for virtual Compton scattering one knows that $g_{1,2}(x) = 0$ for $|x| > 1$ and that $g_{1,2}(-x) = g_{1,2}(x)$. Consequently if we define the n th moment of $g_{1,2}(x)$ by $\int_0^1 dx x^{n-1} g_{1,2}(x) dx$ and we substitute the field-theoretic expressions from (11.5.40), (11.5.38), (11.5.46) and (11.5.48), we can extend the integration region to $-\infty \leq x \leq \infty$ so that integration over x in (11.5.38) and (11.5.48) will produce a δ -function $\delta(\tau)$. Subsequently performing the integral over τ will turn the bilocal operator products in (11.5.39) and (11.5.49) into a product of *local* operators. (Note that we are

interchanging orders of integration so some care may be needed regarding convergence questions.) Powers of x can be turned into derivatives with respect to τ . Proceeding in this way one ends up with expressions for the odd moments of $g_{1,2}(x)$ and the even moments of what can be considered the *valence* parts of $g_{1,2}(x)$, in terms of hadronic matrix elements of local operators (Efremov, Leader and Teryaev, 1997).

The most important result of the latter type is the so-called ELT sum rule, involving the valence parts (V) of g_1 and g_2 :

$$\int_0^1 [g_1^V(x) + 2g_2^V(x)] x dx = 0 \tag{11.6.1}$$

This is unusual in that, like the Bjorken sum rule to be discussed below, it is a rigorous result. Testing the sum rule requires data on both protons and neutrons. Unfortunately the data on $g_2(x)$ are not yet accurate enough for a significant test.

In the operator product approach one begins with an expression for $W_{\mu\nu}$ in terms of the commutator of electromagnetic currents, which can be deduced from the Feynman diagram Fig. 11.1 to be

$$W_{\mu\nu}(q; P, \mathcal{S}) = \frac{1}{2\pi} \int d^4x e^{iq \cdot x} \langle P, \mathcal{S} | [J_\mu(x), J_\nu(0)] | P, \mathcal{S} \rangle \tag{11.6.2}$$

and which implies that it is, up to a numerical factor, the imaginary part of the tensor $T_{\mu\nu}$ that appears in the expression $\epsilon^{\mu*} T_{\mu\nu} \epsilon^\nu$ for the forward virtual-photon Compton scattering amplitude.

The behaviour of $W_{\mu\nu}$ in the deep inelastic limit is controlled by the behaviour of the product of currents near the light cone $x^2 = 0$ and can be derived from Wilson’s operator product expansion. A lengthy analysis is needed involving the use of dispersion relations for forward virtual Compton scattering and leads to expressions for the odd moments only.

In either approach, keeping only the leading *twist*¹ operators, which give the dominant contribution in the Bjorken limit, the final result for the moments has the form

$$\int_0^1 dx x^{n-1} g_1(x, Q^2) = \frac{1}{2} \sum_i \delta_i a_n^i E_{1,i}^n(Q^2, g) \quad n = 1, 3, 5, \dots \tag{11.6.3}$$

and

$$\int_0^1 dx x^{n-1} g_2(x, Q^2) = \frac{1-n}{2n} \sum_i \delta_i [a_n^i E_{1,i}^n(Q^2, g) - d_n^i E_{2,i}^n(Q^2, g)] \tag{11.6.4}$$

$n = 3, 5, 7, \dots$

¹ Twist is defined as the mass dimension of an operator minus its spin.

where the δ_i are numerical coefficients, the $E_i^n(Q^2, g)$ are *coefficient functions* that can be calculated perturbatively in the strong coupling constant g and the a_n^i and d_n^i are related to the hadronic matrix elements of the local operators. The label i indicates what kind of operator is contributing: for flavour-non-singlet operators, only quark fields and their covariant derivatives occur and $i = 1, \dots, 8$ corresponds to the components of an $SU(3)$ octet of flavours; for the flavour-singlet case, $i = \Psi$ or G corresponds to flavour-singlet combinations of quark operators or gluon operators respectively (and their covariant derivatives).

For details and for a discussion of the tantalizing question whether it is permissible to put $n = 1$ in (11.6.4), thereby obtaining the Burkhardt–Cottingham sum rule

$$\int_0^1 dx g_2(x, Q^2) = 0 \tag{11.6.5}$$

the reader may consult Anselmino, Efremov and Leader (1995). The data on $g_2(x, Q^2)$ are not yet accurate enough for a significant test of (11.6.5).

Here we shall concentrate on the very interesting question of the first moment of $g_1(x, Q^2)$, because it is related to the puzzle about the spin content of the nucleon. In this case (11.6.3) can be written, for the proton, as

$$\Gamma_1^p(Q^2) \equiv \int_0^1 dx g_1^p(x, Q^2) \tag{11.6.6}$$

$$= \frac{1}{12} \left[\left(a_3 + \frac{a_8}{\sqrt{3}} \right) E_{\text{NS}}(Q^2) + \frac{4}{3} a_0(Q^2) E_{\text{S}}(Q^2) \right] \tag{11.6.7}$$

where the non-singlet and singlet coefficient functions have the expansion¹

$$E_{\text{NS}}(Q^2) = 1 - \frac{\alpha_s}{\pi} - \left(\frac{3.58}{3.25} \right) \left(\frac{\alpha_s}{\pi} \right)^2 \dots \tag{11.6.8}$$

$$E_{\text{S}}(Q^2) = 1 - \frac{\alpha_s}{\pi} - \left(\frac{1.10}{-0.07} \right) \left(\frac{\alpha_s}{\pi} \right)^2 \dots \tag{11.6.9}$$

where $\alpha_s = \alpha_s(Q^2)$ is the running QCD coupling and the upper and lower numbers correspond to taking either three flavours of quark or four flavours if one includes the charm quark.

In the above, a_3 and a_8 are measures of the proton matrix elements of an $SU(3)$ flavour octet of quark axial-vector currents:

$$\langle P, \mathcal{S} | J_{5\mu}^j | P, \mathcal{S} \rangle = M a_j \mathcal{S}_\mu \quad j = 1, \dots, 8 \tag{11.6.10}$$

¹ These coefficients are ‘scheme dependent’ (see Section 11.7) and the result quoted corresponds to the $\overline{\text{MS}}$ scheme.

where

$$J_{5\mu}^j = \bar{\psi} \gamma_\mu \gamma_5 \left(\frac{\lambda_j}{2} \right) \psi. \quad (11.6.11)$$

Here the λ_j are the usual Gell-Mann matrices and ψ is a column vector in flavour space,

$$\psi = \begin{pmatrix} \psi_u \\ \psi_d \\ \psi_s \end{pmatrix}. \quad (11.6.12)$$

The coefficient a_0 in (11.6.7) is a measure of the flavour-singlet operator. Now in (11.6.3), for $n \geq 2$ there are both gluonic and quarkonic flavour-singlet operators but for $n = 1$, the case we are now considering, the OPE has only one operator, the quark flavour-singlet current

$$J_{5\mu}^0 = \bar{\psi} \gamma_\mu \gamma_5 \psi \quad (11.6.13)$$

and a_0 is defined by

$$\langle P, \mathcal{S} | J_{5\mu}^0 | P, \mathcal{S} \rangle = 2M a_0 \mathcal{S}_\mu. \quad (11.6.14)$$

The absence of a gluonic operator in the first moment of g_1 will turn out to be a non-trivial issue.

To the extent that flavour $SU(3)$ is a global symmetry of the strong interactions the non-singlet octet of currents will be conserved currents, and this will lead to the a_j ($j = 1, \dots, 8$) being independent of Q^2 . The singlet current is not conserved, as a consequence of the axial anomaly (Adler, 1969; Bell and Jackiw, 1969), so that a_0 depends on Q^2 . (This will be discussed in subsection 11.6.2.)

Now what is remarkable is that the octet of axial-vector currents (11.6.11) is precisely the set of currents that controls the weak β -decays of the neutron and of the spin-1/2 hyperons. Consequently a_3 and a_8 can be expressed in terms of two parameters F and D measured in hyperon β -decay (see, for example, Chapter 4 of Bailin, 1982):

$$a_3 = F + D \equiv g_A = 1.2573 \pm 0.0028 \quad (11.6.15)$$

$$\frac{1}{\sqrt{3}} a_8 = \frac{1}{3}(3F - D) = 0.193 \pm 0.008. \quad (11.6.16)$$

It follows that the measurement of $\Gamma_1^p(Q^2)$ in polarized DIS can be interpreted, via (11.6.7), as a measurement of $a_0(Q^2)$.

The determination of $\Gamma_1^p(Q^2)$ is not entirely straightforward, firstly since extrapolations of the data on $g_1(x, Q^2)$ have to be made to the regions $x = 0$ and $x = 1$ in calculating the integral in (11.6.6) and secondly because the data at different x -values correspond to different ranges of Q^2 . At present the value of Γ_1^p at $Q^2 = 10$ (GeV/c)² is believed to lie in the range

$$0.130 \leq \Gamma_1^p(Q^2 = 10 \text{ (GeV/c)}^2) \leq 0.142 \quad (11.6.17)$$

which leads to

$$0.22 \leq a_0(Q^2 = 10 \text{ (GeV}/c)^2) \leq 0.34. \quad (11.6.18)$$

In the famous EMC experiment the measured value of a_0 was consistent with zero and led to a ‘crisis in the parton model’ (Leader and Anselmino, 1988). The present value measured of a_0 is still disturbingly small.

Before turning to discuss this intriguing question, note that in going from the case of a proton to a neutron, a_8 and a_0 in (11.6.7) remain unchanged whereas a_3 reverses its sign. Consequently one has the *Bjorken sum rule*:

$$\int_0^1 dx [g_1^p(x, Q^2) - g_1^n(x, Q^2)] = \frac{g_A}{6} E_{\text{NS}}(Q^2). \quad (11.6.19)$$

This is considered to be a very fundamental result. Moreover the right-hand side is known to great accuracy (see (11.6.15)) and much effort has gone into trying to test (11.6.19). Up to the present (11.6.19) seems to be well satisfied by the data, as will be discussed in Section 11.8.

11.6.1 A spin crisis in the parton model

In the naive parton model the nucleon is simply an ensemble of free, parallel-moving quarks. The picture can be recovered by putting the QCD coupling g equal to zero. In that case the quark fields in $J_{5\mu}^0$ in (11.6.13) and (11.6.11) become free fields, and treating the nucleon state in (11.6.14) as a superposition of free-quark states one easily finds that

$$a_0 = \Delta\Sigma \equiv \int_0^1 \Delta\Sigma(x) dx \quad (11.6.20)$$

where

$$\Delta\Sigma(x) \equiv \Delta u(x) + \Delta\bar{u}(x) + \Delta d(x) + \Delta\bar{d}(x) + \Delta s(x) + \Delta\bar{s}(x). \quad (11.6.21)$$

Now given the physical significance of the number densities $q_{\pm}(x)$ discussed in Section 11.4 it is clear that the integral in (11.6.20) is just twice the expectation value of the sum of the z -components of the quark and antiquark spins, i.e.

$$a_0 = \Delta\Sigma = 2 \langle S_z^{\text{quarks}} \rangle, \quad (11.6.22)$$

which implies, if we adopt (11.1.1) uncritically, that we expect $a_0 \approx 1$.

As mentioned, the EMC experiment found a_0 compatible with zero provoking a ‘crisis in the parton model’ and the present value, given in (11.6.18), is still small compared with naive expectations. It is not clear how to quantify the extent to which we expect a_0 to differ from its naive value, but it is generally felt that the small value in (11.6.18) is not in accord with intuition.

We shall see in the next section that (11.6.20) and hence (11.6.22) are, surprisingly, not correct in the interacting theory.

11.6.2 The gluon anomaly

Consider the axial current

$$J_{5\mu}^f = \bar{\psi}_f(x)\gamma_\mu\gamma_5\psi_f(x) \quad (11.6.23)$$

made up of quark operators of definitive flavour f (an implicit colour sum is always implied). From the free Dirac equation of motion one finds that

$$\partial^\mu J_{5\mu}^f = 2im_q\bar{\psi}_f(x)\gamma_5\psi_f(x) \quad (11.6.24)$$

where m_q is the mass of the quark of flavour f . In the chiral limit $m_q \rightarrow 0$ (11.6.24) appears to imply that $J_{5\mu}^f$ is conserved. If this were really true then there would be a symmetry between left- and right-handed quarks, leading to a parity degeneracy of the hadron spectrum, e.g. there would exist two protons of opposite parity. However, the formal argument from the free equations of motion is not reliable and there is an anomalous contribution from the triangle diagram shown in Fig. 11.11, where two gluons couple to the current of (11.6.23).

As a consequence the axial current is not conserved when $m_q = 0$. One has instead, for the QCD case,

$$\partial^\mu J_{5\mu}^f = \frac{\alpha_s}{4\pi} G_{\mu\nu}^a \tilde{G}_a^{\mu\nu} \quad (11.6.25)$$

where $\tilde{G}_a^{\mu\nu}$ is the dual field tensor

$$\tilde{G}_a^{\mu\nu} \equiv \frac{1}{2}\epsilon^{\mu\nu\rho\sigma}G_{\rho\sigma}^a. \quad (11.6.26)$$

The result (11.6.25), which emerges from a calculation of the triangle diagram using $m_q = 0$ and the gluon virtuality $k^2 \neq 0$, is really a particular

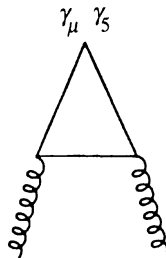


Fig. 11.10. Triangle diagram giving rise to the gluon anomaly.

limit of a highly non-uniform function. If we take $m_q \neq 0, k^2 \neq 0$ the right-hand side of (11.6.25) is multiplied by

$$T(m_q^2/k^2) = 1 - \frac{2m_q^2/k^2}{\sqrt{1 + 4m_q^2/k^2}} \ln \left(\frac{\sqrt{1 + 4m_q^2/k^2} + 1}{\sqrt{1 + 4m_q^2/k^2} - 1} \right). \tag{11.6.27}$$

We see that on the one hand the gluon anomaly corresponds to $T \rightarrow 1$ for $m_q^2/k^2 \rightarrow 0$. On the other hand, for on-shell gluons $k^2 = 0$ and $m_q \neq 0$, i.e. in the limit $m_q^2/k^2 \rightarrow \infty$ the terms cancel, $T \rightarrow 0$ and there is no anomaly. In our case the gluons are strictly speaking, bound inside the proton so they are off shell and $k^2 \neq 0$ is the relevant case.

The anomaly induces an effectively point-like interaction between $J_{\mu 5}^0$ and gluons. Using the expression given in Adler (1969), generalized to QCD, the matrix element of $J_{\mu 5}^0$ between almost free gluons is

$$\langle k; \lambda | J_{5\mu}^f | k; \lambda \rangle = \frac{i\alpha_s}{2\pi} \epsilon_{\mu\nu\rho\sigma} k^\nu \epsilon^{*\rho}(\lambda) \epsilon^\sigma(\lambda) T(m_q^2/k^2);$$

this, via (3.4.28) and (3.1.80), becomes

$$\langle k; \lambda | J_{5\mu}^f | k; \lambda \rangle = -\frac{\alpha_s}{2\pi} \mathcal{S}_\mu^{\text{gluons}}(k, \lambda) T(m_q^2/k^2), \tag{11.6.28}$$

where λ is the gluon helicity and we may take

$$\mathcal{S}_\mu^{\text{gluons}}(k, \lambda) \approx \lambda k_\mu$$

as the covariant spin vector for almost massless gluons.

The component of the proton wave function containing almost free gluons then yields a gluonic contribution to a_0

$$a_0^{\text{gluons}}(Q^2) = -3 \frac{\alpha_s}{2\pi} \Delta G(Q^2) \tag{11.6.29}$$

where

$$\Delta G(Q^2) \equiv \int_0^1 \Delta G(x, Q^2) dx. \tag{11.6.30}$$

Here $\Delta G(x)$ is the analogue for gluons of $\Delta q(x)$. The concept of Q^2 -dependent parton distributions such as $\Delta G(x, Q^2)$ is explained in Section 11.7. The factor 3 in (11.6.29) arises from taking $m_u, m_d, m_s \ll k^2, m_c, m_b, m_t \gg k^2$ so that $T = 1$ for m_u, m_d, m_s and $T = 0$ for m_c, m_b, m_t .

Instead of (11.6.20) we now have (Efremov and Teryaev, 1988; Altarelli and Ross, 1988; Carlitz, Collins and Mueller, 1988; Anselmino and Leader, 1988)

$$a_0(Q^2) = \Delta \Sigma - \frac{3\alpha_s(Q^2)}{2\pi} \Delta G(Q^2). \tag{11.6.31}$$

The result (11.6.31) is remarkable. It shows that there is a gluonic contribution to the first moment of g_1 . Moreover it is quite anomalous in

the sense that it look like a perturbative correction that will disappear at large Q^2 , where $\alpha_s(Q^2) \rightarrow 0$, but in reality does not do so because $\Delta G(Q^2)$ can be shown to grow in precisely the right way to compensate for the decrease of $\alpha_s(Q^2)$. It also has the fundamental implication that *the small measured value of a_0 does not necessarily imply that $\Delta\Sigma$ is small.*

So, for example, we could let the quarks carry 60% of the proton's spin at $Q^2 = 10 \text{ (GeV/c)}^2$ and the experimental value (11.6.18) would then imply

$$2.2 \leq \Delta G(Q^2 = 10 \text{ (GeV/c)}^2) \leq 3.3. \tag{11.6.32}$$

Now similarly to (11.6.22), $\Delta G(Q^2)$ measures the contribution to the proton's spin arising from the spin of the gluon constituents. Bearing in mind (11.1.1) we have the apparently surprising result that

$$\langle S_z^{\text{gluons}}(Q^2 = 10 \text{ (GeV/c)}^2) \rangle \approx 2 \sim 3.$$

However, the operator corresponding to the spin of a gluon is not a conserved operator, so its matrix elements depend upon the renormalization scale (this causes the Q^2 -dependence) and $\langle S_z^G(Q^2) \rangle$ does not have a simple physical interpretation as a fixed number. Indeed $\langle S_z^G(Q^2) \rangle \rightarrow \infty$ as $Q^2 \rightarrow \infty$ and this is compensated by the fact that the gluon *orbital* angular momentum grows in the opposite sense:

$$\langle L_z^{\text{gluons}}(Q^2) \rangle \rightarrow -\infty \quad \text{as} \quad Q^2 \rightarrow \infty.$$

Given that gluons play no rôle in the low energy constituent quark model, it is somewhat reassuring that the above value of $\langle S_z^{\text{gluons}} \rangle$ at $Q^2 = 10 \text{ (GeV/c)}^2$ leads, via a perturbative calculation, to

$$\langle S_z^{\text{gluons}}(Q^2 = 4\Lambda_{\text{QCD}}^2) \rangle \lesssim 0.6.$$

Below this value of Q^2 we enter the non-perturbative regime so cannot estimate how $\langle S_z^{\text{gluons}} \rangle$ behaves.

In contrast to this, $\Delta\Sigma$ or $\langle S_z^{\text{quarks}} \rangle$ can be linked to a conserved operator (see Anselmino, Efremov and Leader, 1995, Section 6.3) and so are independent of Q^2 . It thus makes sense to expect that $\Delta\Sigma \approx 1$.

11.7 QCD corrections and evolution

The field-theoretic approach of Section 11.5 leads to the simple parton model when the hard scattering amplitude E in Fig. 11.4 is treated in the Born approximation and the quark fields as free fields. When gluonic corrections are included, problems arise from the so-called *mass or collinear singularities* linked to the effective masslessness of the partonic quarks. A subtle process of *factorization at scale μ* (chosen for simplicity to be the

same as the renormalization scale) allows the singular terms to be absorbed into the non-calculable parton distribution functions. These then depend on μ , leaving the finite terms as Q^2 -dependent correction terms in the expressions for the structure functions, which thus no longer obey exact Bjorken scaling. In fact they develop a slow logarithmic dependence on Q^2 .

In the *leading logarithmic approximation* (LLA) one keeps only the most dominant terms, proportional to $\alpha_s \ln(Q^2/\mu^2)$, and finds that the parton-model expressions remain valid provided the replacements

$$q(x) \rightarrow q(x, Q^2) \quad \Delta q(x) \rightarrow \Delta q(x, Q^2) \quad (11.7.1)$$

to the Q^2 -dependent parton distributions are made.

In this approximation the $q(x, Q^2)$ and $\Delta q(x, Q^2)$ are universal, i.e. they are a property of the nucleon and will appear in any hard reaction involving the nucleon.

The x -dependence of the $\Delta q(x, Q^2)$ cannot be calculated, of course, but the variation with Q^2 is controlled by the Gribov, Lipatov, Altarelli and Parisi *evolution equations* (Gribov and Lipatov, 1972; Altarelli and Parisi, 1977), which have the generic form

$$\frac{d}{d \ln Q^2} \Delta q(x, Q^2) = \frac{\alpha_s(Q^2)}{2\pi} \int_x^1 \frac{dy}{y} \left\{ \Delta P_{qq}^{(0)}(x/y) \Delta q(y, Q^2) + \Delta P_{qG}^{(0)} \Delta G(y, Q^2) \right\} \quad (11.7.2)$$

$$\frac{d}{d \ln Q^2} \Delta G(x, Q^2) = \frac{\alpha_s(Q^2)}{2\pi} \int_x^1 \frac{dy}{y} \left\{ \Delta P_{Gq}^{(0)}(x/y) \Delta q(y, Q^2) + \Delta P_{GG}^{(0)}(x/y) \Delta G(y, Q^2) \right\} \quad (11.7.3)$$

The $\Delta P_{ij}^{(0)}$ are the lowest-order *polarized splitting functions*, first given for QCD in Altarelli and Parisi (1977).

11.7.1 Beyond leading order; scheme dependence

When the *non-dominant* correction terms are included and when one works to order α_s^2 , i.e. to the next-to-leading order (NLO), two new features arise.

(1) The expression for $g_1(x, Q^2)$ in (11.4.5) is modified to

$$g_1(x, Q^2) = \frac{1}{2} \sum_q e_q^2 \left\{ \Delta q(x, Q^2) + \Delta \bar{q}(x, Q^2) + \frac{\alpha_s(Q^2)}{2\pi} \int_x^1 \frac{dy}{y} \left[\Delta C_q(x/y) \left[\Delta q(y, Q^2) + \Delta \bar{q}(y, Q^2) \right] + \Delta C_G(x/y) \Delta G(y, Q^2) \right] \right\} \quad (11.7.4)$$

where the sum is over the *flavours* of the quarks and antiquarks and the *coefficient functions* ΔC_q , ΔC_G are related to calculable short-distance, i.e. hard, photon–quark and photon–gluon cross-sections. Figure 11.12 shows the mechanism whereby the photon couples to the gluon. The convolutions in (11.7.4) are often symbolized by $\Delta C_q \otimes \Delta q$, $\Delta C_G \otimes \Delta G$ etc. and have the property that the moment of the convolution is the product of the moments of the functions: $(f \otimes g)^{(n)} = f^{(n)}g^{(n)}$.

At this order the evolution equations have the form of (11.7.2) and (11.7.3) but the splitting functions, now calculated to higher order, have the form

$$\Delta P_{ij} = \Delta P_{ij}^{(0)} + \frac{\alpha_s}{2\pi} \Delta P_{ij}^{(1)}.$$

All these functions are given in a very clear form in Vogelsang (1996).

(2) The massive calculations involved are plagued by ambiguities linked to the renormalization of operators containing γ_5 . In *any* theory requiring infinite renormalization the subtraction of the infinite terms is clearly defined, but the handling of associated finite terms is a matter of taste, giving rise to a *renormalization-scheme dependence* of the auxiliary quantities in any calculation. Physically measurable quantities, like g_1 for example, must be independent of the choice of scheme. But in NLO the coefficient functions, and therefore the parton distributions, become scheme dependent and one must specify in what scheme one is working.

For the unpolarized case this is straightforward and there are simple unambiguous ways to define the various schemes in use, DIS, MS (minimal subtraction), $\overline{\text{MS}}$ etc. Moreover the parton distributions in the various schemes differ from each other only by terms of order $\alpha_s(Q^2)$. In the polarized case, because of the complexity of the calculations one often renormalizes using the modern *dimensional regularization* technique (for a simple introduction, see Leader and Predazzi, 1996, Vol. 2) and it then turns out that specifying the finite subtractions as MS or $\overline{\text{MS}}$ is not enough

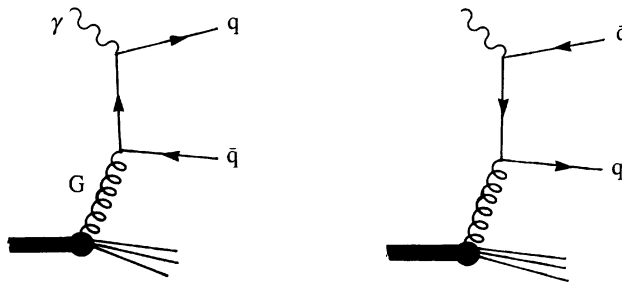


Fig. 11.11 Diagram illustrating how the photon couples to the gluon in the nucleon.

– there remain ambiguities linked to the freedom in defining γ_5 in more than four-dimensions.

The classic method of handling γ_5 , due to 't Hooft and Veltman (1972) and to Breitenlohner and Maison (1977), leads to what we shall label the $\overline{\text{MS}}$ –HVBM scheme. But this has the undesirable peculiarity that the renormalized isovector current $J_{\mu 5}^3$, see eqn (11.6.11), is *not* conserved.

The main schemes in use are:

- (1) a modified $\overline{\text{MS}}$ –HVBM scheme, due to Mertig and van Neerven (1996) and to Vogelsang (1996), which does conserve $J_{\mu 5}^3$ and which we shall refer to as the $\overline{\text{MS}}$ –MNV *scheme*;
- (2) a scheme referred to as the *AB scheme* in Ball, Forte and Ridolfi (1996), which modifies only the first moment of $\Delta\Sigma(x, Q^2)$, so as to make it independent of Q^2 ;
- (3) the more physically motivated scheme advocated by Carlitz, Collins and Mueller (1988), by Anselmino, Efremov and Leader (1995) and, on the basis of more general arguments, by Teryaev and Müller (1997). This has the advantage that the contribution to $g_1(x, Q^2)$ arising from the reaction virtual-photon $+p \rightarrow \text{jet}(\mathbf{k}_T) + \text{jet}(-\mathbf{k}_T) + X$ (see Fig. 11.11), for the production of two jets with *large* transverse momentum \mathbf{k}_T , is directly given by the gluon term in (11.7.4) with, clearly, the coefficient function appropriate to this scheme, which is given below. We shall label this the *JET scheme*. Of course, this scheme also has the desirable property that the first moment of $\Delta\Sigma(x, Q^2)$ is independent of Q^2 .

The most important difference between these schemes shows up in the first moment of g_1 . One finds that

$$\int_0^1 dx \Delta C_G^{\overline{\text{MS}}\text{-MNV}}(x) = 0 \quad (11.7.5)$$

so that the gluon makes no contribution to the first moment of g_1 . Thereby one loses the nice explanation given by (11.6.31) for the smallness of a_0 . Moreover the first moment of the quark-singlet combination, $\Delta\Sigma^{\overline{\text{MS}}\text{-MNV}}(Q^2)$, varies with Q^2 so cannot be compared with the constituent quark result (11.1.1).

On the contrary, in the AB and JET schemes one has

$$\int_0^1 dx \Delta C_G^{\text{AB}}(x) = \int_0^1 dx \Delta C_G^{\text{JET}}(x) = -1 \quad (11.7.6)$$

in exact agreement with the result for a_0 in (11.6.31). Moreover the quark-

singlet-contribution first moment, $\Delta\Sigma^{\text{AB}} = \Delta\Sigma^{\text{JET}}$, is independent of Q^2 , allowing an intuitive interpretation as the spin carried by the quarks. For reasons explained earlier we feel the JET scheme has a more direct physical interpretation than the AB scheme.

There is another strange feature peculiar to the polarized case. The gluon distributions are the same in the $\overline{\text{MS}}$ -MNV, AB and JET schemes, but the first moments of the singlet quark densities are related by

$$\Delta\Sigma^{\text{AB}} = \Delta\Sigma^{\text{JET}} = \Delta\Sigma^{\overline{\text{MS}}\text{-MNV}}(Q^2) + \frac{1}{3} \frac{\alpha_s(Q^2)}{2\pi} \Delta G(Q^2) \quad (11.7.7)$$

so that, as explained after eqn (11.6.31), the difference between them is not really of order $\alpha_s(Q^2)$ and could be quite large. Scheme changes of this type are thus quite anomalous compared with the unpolarized case.

In the JET scheme the coefficient $\Delta C_G(x)$ appearing in the expression (11.7.4) for $g_1(x, Q^2)$ is given by

$$\Delta C_G^{\text{JET}}(x) = (2x - 1) \left[\ln \left(\frac{1-x}{x} \right) - 1 \right] \quad (11.7.8)$$

and $\Delta C_q(x)$ is the same in both types of scheme.

In NLO the quark non-singlet distributions are actually of two kinds, combinations like $(\Delta u + \Delta \bar{u}) - (\Delta d + \Delta \bar{d})$, which are genuinely *flavour non-singlets*, and combinations like $(\Delta u - \Delta \bar{u}) \equiv \Delta u_V$, which are *valence non-singlets*. These have different evolution properties, as explained in Vogelsang (1996). In comparing the $\overline{\text{MS}}$ -MNV, AB and JET schemes, we find that all non-singlet distributions are the same in these schemes. Also the gluon density is the same. Only the singlet quark density $\Delta\Sigma(x, Q^2)$ changes. For any scheme change of this type, one has

$$\begin{aligned} \Delta\Sigma(x, Q^2)|_{\text{new}} &= \Delta\Sigma(x, Q^2)|_{\overline{\text{MS}}\text{-MNV}} \\ &+ \frac{N_f}{2} \frac{\alpha_s(Q^2)}{2\pi} h_G \otimes \Delta G \end{aligned} \quad (11.7.9)$$

where $h_G(x)$ is a function specifying the change; for the transformation $\overline{\text{MS}}$ -MNV \rightarrow JET one has

$$h_G(x) = 4(1-x). \quad (11.7.10)$$

Of course the NLO part of the splitting functions, which control the evolution in (11.7.2) and (11.7.3), is different in the two schemes. The connection is given by

$$\begin{aligned} \left(\Delta P_{qq}^{\text{PS}} \right)_{\text{new}} &= \left(\Delta P_{qq}^{\text{PS}} \right)_{\overline{\text{MS}}\text{-MNV}} \\ &+ \frac{N_f}{2} \frac{\alpha_s}{2\pi} h_G \otimes \Delta P_{Gq}^{(0)} \end{aligned} \quad (11.7.11)$$

$$\begin{aligned}
 (\Delta P_{qG})_{\text{new}} &= (\Delta P_{qG})_{\overline{\text{MS}}\text{-MNV}} + \frac{N_f \alpha_s}{2 \ 2\pi} \\
 &\quad \times \left[h_G \otimes \left(\Delta P_{GG}^{(0)} - \Delta P_{qq}^{(0)} \right) - \frac{\beta_0}{2} h_G \right] \quad (11.7.12)
 \end{aligned}$$

$$(\Delta P_{Gq})_{\text{new}} = (\Delta P_{Gq})_{\overline{\text{MS}}\text{-MNV}} \quad (11.7.13)$$

$$(\Delta P_{GG})_{\text{new}} = (\Delta P_{GG})_{\overline{\text{MS}}\text{-MNV}} - \frac{N_f \alpha_s}{2 \ 2\pi} h_G \otimes \Delta P_{Gq}^{(o)} \quad (11.7.14)$$

where

$$\beta_0 = 11 - 2N_f/3. \quad (11.7.15)$$

For the case $\overline{\text{MS}}\text{-MNV} \rightarrow \text{JET}$ these simplify to

$$\begin{aligned}
 (\Delta P_{qq}^{PS})_{\text{JET}} &= (\Delta P_{qq}^{PS})_{\overline{\text{MS}}\text{-MNV}} \\
 &\quad - 8 \frac{N_f \alpha_s}{3 \ 2\pi} [(x+2) \ln x + 3(1-x)] \quad (11.7.16)
 \end{aligned}$$

$$\begin{aligned}
 (\Delta P_{qG})_{\text{JET}} &= (\Delta P_{qG})_{\overline{\text{MS}}\text{-MNV}} + 4 \frac{N_f \alpha_s}{3 \ 2\pi} \\
 &\quad \times \{ 5(1-x) [\ln(1-x) - 7] \\
 &\quad - (11x + 16) \ln x \} \quad (11.7.17)
 \end{aligned}$$

$$(\Delta P_{Gq})_{\text{JET}} = (\Delta P_{Gq})_{\overline{\text{MS}}\text{-MNV}} \quad (11.7.18)$$

$$\begin{aligned}
 (\Delta P_{GG})_{\text{JET}} &= (\Delta P_{GG})_{\overline{\text{MS}}\text{-MNV}} \\
 &\quad + 8 \frac{N_f \alpha_s}{3 \ 2\pi} [(x+2) \ln x - 3(1-x)] \quad (11.7.19)
 \end{aligned}$$

Note that the connection between the n th moments following from (11.7.9) is

$$\begin{aligned}
 \Delta \Sigma^{(n)}(Q^2)|_{\text{JET}} &= \Delta \Sigma^{(n)}(Q^2)|_{\overline{\text{MS}}\text{-MNV}} \\
 &\quad + N_f \frac{\alpha_s(Q^2)}{2\pi} \frac{2}{n(n+1)} \Delta G^{(n)}(Q^2). \quad (11.7.20)
 \end{aligned}$$

We remind the reader that detailed expressions for all the $\overline{\text{MS}}\text{-MNV}$ functions can be found in Vogelsang (1996). A study of scheme dependence in the analysis of data is given in Leader, Sidorov and Stamenov (1998b).

11.8 Phenomenology: the polarized-parton distributions

Pioneering experiments with polarized electron beams and polarized proton targets at SLAC in the 1970s demonstrated significant spin dependence, but it was not until the surprising results of the EMC experiment in 1988 that the field really took off. A vast programme of experiments has been, and is, under way at CERN (the SMC group), at SLAC (experiments E 142, 143, 154, 155) and at HERA (the HERMES collaboration)

and precision data on the polarized structure function g_1 is available for protons, neutrons and deuterons over a reasonable range of x and Q^2 . Data on g_2 have recently begun to be published. For access to the experimental literature, see Abe *et al.* (1997a).

Several NLO analyses of the data have been carried out during the last year or two, leading to much improved information on the polarized parton densities (Glück, Reya, Stratmann and Vogelsang, 1996; Ball, Forte and Ridolfi, 1996; Abe *et al.*, 1997b; Altarelli *et al.*, 1997; Leader, Sidorov and Stamenov, 1998a, 1999).

However, it would be wrong to imagine that the polarized densities can now be determined to the same accuracy with which the unpolarized densities are known. This can be understood quite simply. Up to the present the polarized data consist solely of fully inclusive neutral current (in effect, photon-induced) reactions on nucleons, i.e. one has information on two polarized structure functions $g_1^p(x, Q^2)$ and $g_1^n(x, Q^2)$. Even if one makes some simplifying assumptions about the polarized sea, one is still expressing two experimental functions in terms of four densities $\Delta u, \Delta d, \Delta \bar{q}$ and ΔG . What is lacking here is information from charged current reactions, which play an important rôle in pinning down the unpolarized densities. Neutrino experiments on a polarized target have been inconceivable up to now and charged current reactions of the type $ep \rightarrow \nu X$ will be extremely difficult. The situation is somewhat alleviated by the constraints coming from the beautiful connection between the first moments of the polarized parton densities and weak interaction physics, as discussed in Section 11.6; see eqns (11.6.15) and (11.6.16). For one has

$$a_3 = \int_0^1 dx \left[\Delta u(x, Q^2) + \Delta \bar{u}(x, Q^2) - \Delta d(x, Q^2) - \Delta \bar{d}(x, Q^2) \right] \quad (11.8.1)$$

and

$$a_8 = \frac{1}{\sqrt{3}} \int_0^1 dx \left[\Delta u(x, Q^2) + \Delta \bar{u}(x, Q^2) + \Delta d(x, Q^2) + \Delta \bar{d}(x, Q^2) - 2\Delta s(x, Q^2) - 2\Delta \bar{s}(x, Q^2) \right]. \quad (11.8.2)$$

In all analyses one chooses some parametrization for the functional form of the distribution at some initial scale Q_0^2 , in terms of a small number of the unknown parameters, and then evolves the distributions up to the values of Q^2 corresponding to the data and determines the parameters by a best fit to the data. A typical parametrization might involve the unpolarized distribution in the generic form

$$\Delta f(x, Q_0^2) = Ax^\alpha(1-x)^\beta f(x, Q_0^2) \quad (11.8.3)$$

where f is the unpolarized version of Δf and where A , α and β are to be determined from the data. Or, in the approach of Brodsky, Burkhardt

and Schmidt (1995), both $f(x, Q_0^2)$ and $\Delta f(x, Q_0^2)$ are parametrized as polynomials in x and a simultaneous fit is made to both the polarized and the unpolarized data.

There seem to be two sensible choices of distribution to parametrize at Q_0^2 :

- (1) $\Delta u + \Delta \bar{u}$, $\Delta d + \Delta \bar{d}$, Δs and ΔG , or
- (2) Δu_V , Δd_V , ΔG , together with some *ansatz* about the sea, e.g. $SU(3)$ -symmetric $\Delta \bar{u} = \Delta \bar{d} = \Delta s$ or a weighting in favour of the lightest quarks, e.g. $\Delta \bar{u} = \Delta \bar{d} = \lambda_s \Delta s$, $\lambda_s > 1$. Here $\Delta q_V \equiv \Delta q - \Delta \bar{q}$ are the *valence* parton densities.

In Fig. 11.12 we show recent results on g_1^p from the SMC collaboration. Of great interest is the comparison of their 1996 and 1993 data, especially at small x . We shall discuss this issue in the next section.

In Fig. 11.13 the results on g_1^n from experiments 142 and 154 at SLAC are shown. Here the data are not strictly measured values; they have been evolved to a common value $Q^2 = 5 \text{ (GeV/c)}^2$, but for these experiments this gives only a very small effect. Again, the behaviour at small x raises interesting questions.

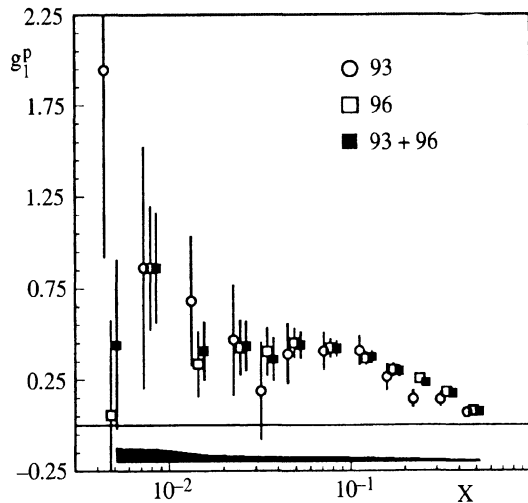


Fig. 11.12 SMC data on $g_1^p(x, Q^2)$ at the measured Q^2 for each x and comparing 1996 and 1993 data. The solid band indicates the systematic uncertainty. ‘93 + 96’ means a weighted average of the two sets of results. (From Adeva *et al.*, 1997.)

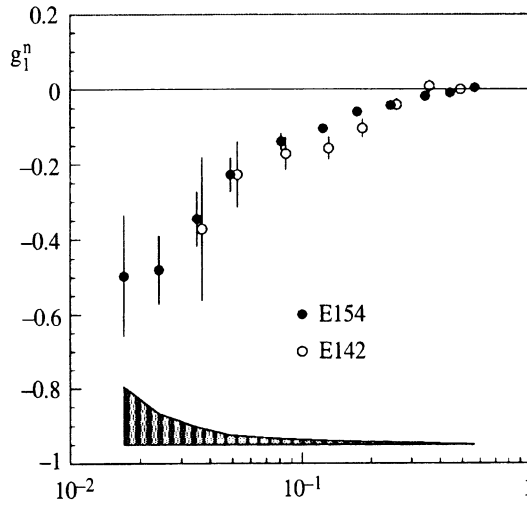


Fig. 11.13 SLAC data on $g_1^n(x, Q^2)$ from experiments E142 and the later E154. The data have been evolved to a common value $Q^2 = 5 \text{ (GeV/c)}^2$ assuming that g_1/F_1 is independent of Q^2 in the range of these measurements. The shaded band indicates the systematic uncertainty. (From Abe *et al.*, 1997c.)

The HERMES group at HERA has recently begun to publish results. An example, comparing their data on g_1^n with the SLAC E142 data, is shown in Fig. 11.15.

In Fig. 11.16 we show typical shapes of the polarized-parton densities at $Q^2 = 4 \text{ (GeV/c)}^2$. In comparing different analyses one finds that on the one hand $\Delta u(x)$ is rather well determined, as is $\Delta d(x)$ for medium

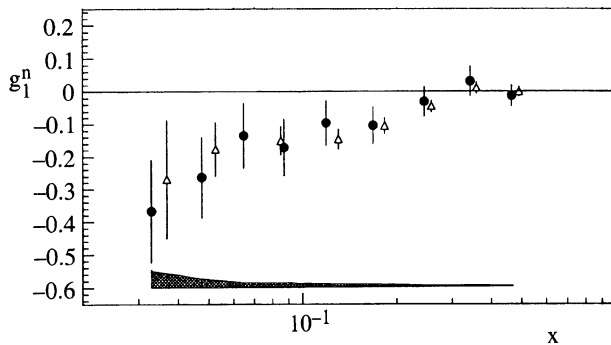


Fig. 11.14 HERMES data on g_1^n , compared with SLAC E142 data: ●, HERMES; △, E142. (From Ackerstaff *et al.*, 1997.)

values of x , but the behaviour of $\Delta d(x)$ for small x and for $x \gtrsim 0.35$ is not yet accurately known. On the other hand the sea-quark distribution is still largely undetermined though it is claimed that there is a tendency to favour an $SU(3)$ flavour symmetric sea. This is quite misleading since *in principle*, this cannot be determined from the data (see Leader, Sidorov and Stamenov, 1998a). Unfortunately the most interesting quantity of all, the gluon distribution $\Delta G(x, Q^2)$, is still relatively poorly determined. That this is so can be understood from the facts that its *direct* contribution to $g_1(x, Q^2)$ is of order $\alpha_s(Q^2)$, see (11.7.4) and that its main rôle is in the evolution equations. However, the range of Q^2 thus far measured is too small for the latter to play a definitive rôle.

In order to give greater weight to the process of evolution, Glück, Reya, Stratmann and Vogelsang (1996) chose the very low value $Q_0^2 = 0.34 \text{ (GeV}/c)^2$ at which to parametrize their initial distributions. One may wonder whether it is meaningful to use perturbative methods at such values of Q^2 , where $\alpha_s(Q^2)$ is relatively large, but there is no doubt that excellent fits to the data were achieved. The same approach was shown to work for the unpolarized case. Stratmann (see Blumlein *et al.*, 1997) claimed that even in this approach $\Delta G(x, Q^2)$ is virtually undetermined. However, a more recent study, including much new and precise data, was shown by Leader, Sidorov and Stamenov (1999) to constrain $\Delta G(x)$ within reasonable limits, as shown in Fig. 11.17.

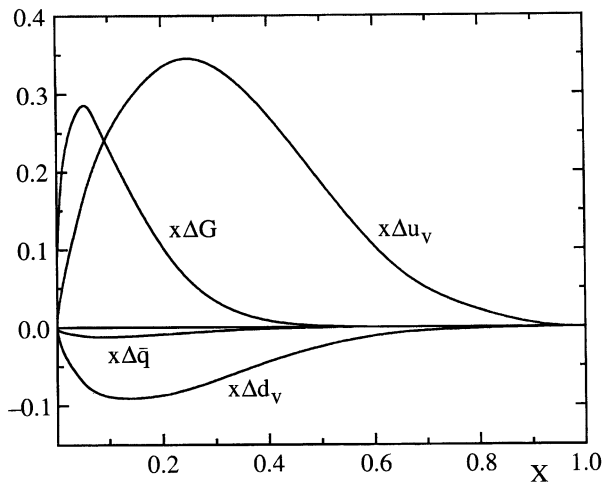
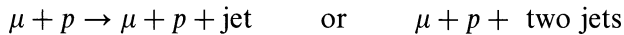


Fig. 11.15 Typical shapes of the polarized-parton densities (multiplied by x) at $Q^2 = 4 \text{ (GeV}/c)^2$, obtained from a NLO analysis assuming an $SU(3)$ -symmetric sea. (From Leader, Sidorov and Stamenov, 1998a.)

A knowledge of $\Delta G(x, Q^2)$ is of great importance for understanding the spin structure of the nucleon, but it is clear that polarized DIS is not the best place to seek this information; future experiments, though, in which the proton beam at HERA is polarized, would cover a larger range of Q^2 and thus have better control over the gluon.

The quest for more precise knowledge about $\Delta G(x, Q^2)$ has inspired a whole new series of experiments involving polarized nucleons, which will begin in the very near future. The COMPASS experiment at CERN will study polarized *semi-inclusive* DIS, where, for example, reactions like



are very sensitive to the gluon distribution. The RHIC collider at Brookhaven will have high energy colliding beams of polarized protons, where reactions like Drell–Yan scattering $pp \rightarrow l^+l^-X$, for lepton pairs with large transverse momentum, are also sensitive to $\Delta G(x, Q^2)$. Both COMPASS and an upgraded HERMES experiment will look at the semi-inclusive production of charm. For further information about these new experiments the reader should consult the paper ‘Towards future measurements of $\Delta G/G$ ’ in the Proceedings of the DESY workshop, *Deep Inelastic Scattering Off Polarized Targets: Theory Meets Experiment* (Blümlein *et al.*, 1997).

11.8.1 Behaviour as $x \rightarrow 0$ and $x \rightarrow 1$

In order to test sum rules one must integrate the experimentally measured $g_{1,2}(x, Q^2)$ from $x = 0$ to $x = 1$ and this inevitably means making a

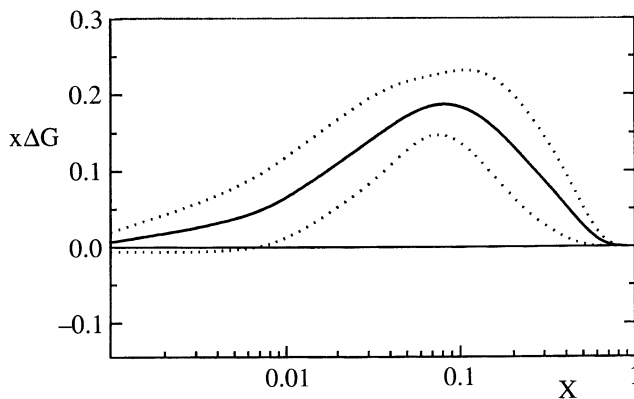


Fig. 11.16 Polarized-gluon density and error band (shown by dotted curves). (From Leader, Sidorov and Stamenov, 1999.)

theoretically biased extrapolation from the region actually covered in the experiment.

In the region $x \rightarrow 1$ there are perturbative QCD arguments (Farrar and Jackson, 1975) that suggest that

$$\frac{\Delta q_V(x)}{q_V(x)} \rightarrow 1 \quad \frac{\Delta \bar{q}(x)}{\bar{q}(x)} \rightarrow 1 \quad \frac{\Delta G(x)}{G(x)} \rightarrow 1. \quad (11.8.4)$$

Even if detailed fits to the data do not always support this behaviour, the disagreement is innocuous from the point of view of the sum rules, since in all cases the parton densities drop rapidly to zero as $x \rightarrow 1$ and the contribution to the sum rule from the large- x region is essentially negligible. Surprisingly, the behaviour as $x \rightarrow 1$ turns out to be quite critical in the analysis of $p^\uparrow p \rightarrow \pi x$ with a transversely polarized proton, is discussed in Section 13.4.

Quite the contrary happens in the region $x \rightarrow 0$, where it is not at all clear what is happening, nor what is expected to happen, theoretically. In view of the connection between DIS and the imaginary part of the forward virtual-photon Compton scattering amplitude (Section 11.6) one would expect the structure functions to have a Regge-type behaviour as the energy $\nu \rightarrow \infty$ at fixed photon ‘mass’ Q^2 . Regge behaviour (see, for example, Collins and Martin, 1984) describes the highly non-perturbative region of forward scattering, so cannot be derived rigorously in QCD, but there are powerful reasons to believe in its validity. In that case we should have at fixed Q^2

$$g_1 \stackrel{\nu \rightarrow \infty}{\approx} \nu^{-\alpha_1} f(Q^2),$$

a behaviour arising from the trajectories associated with the $a_1(1260)$ and $f_1(1285)$ mesons, for which one expects $\alpha_{f_1}(t) \approx \alpha_{a_1}(t)$ and $\alpha_1 \equiv \alpha_{a_1}(0) = -0.14 \pm 0.20$.

Since, via (11.3.15), $\nu \propto 1/x$ we may deduce that, on the one hand, at fixed Q^2

$$g_1(x, Q^2) \stackrel{x \rightarrow 0}{\approx} x^{-\alpha_1} \times (\text{function of } Q^2), \quad (11.8.5)$$

which would imply a rather flat, almost constant behaviour of g_1 as $x \rightarrow 0$. (A detailed analysis of the Regge contributions to DIS is given in Heimann, 1973.)

On the other hand, data on the growth with energy of several exclusive reactions initiated by virtual photons, for example,

$$‘\gamma’ + p \rightarrow p + \text{vector meson},$$

do not seem to follow standard Regge behaviour: they grow much faster with energy ν when Q^2 is significantly different from zero, even though in these reactions $\nu \gg Q$, a condition which used to be thought sufficient

to justify Regge behaviour. Moreover the behaviour of the *unpolarized* structure functions $F_{1,2}(x, Q^2)$ does not seem to follow Regge predictions at small x . This is particularly evident in the HERA data (see, for example, Adloff *et al.*, 1997), where there is a very rapid growth of $F_1(x, Q^2)$, faster than x^{-1} , as $x \rightarrow 0$. This has consequences for the polarized case since there are arguments relating the small- x behaviour of polarized and unpolarized densities, namely, for $x \rightarrow 0$

$$\frac{\Delta q(x)}{q(x)} \propto x \qquad \frac{\Delta G(x)}{G(x)} \propto x$$

which would imply then that $|g_1(x, Q^2)|$ should grow faster than the Regge behaviour (11.8.5) as $x \rightarrow 0$.

Attempts have been made to study the small- x behaviour via a selective summation of terms in perturbation theory. Berera (1992) and Ball, Forte and Ridolfi (1995) studied the small- x behaviour of the evolution equations. Very interesting results emerge. If the starting distribution at Q_0^2 is singular enough as $x \rightarrow 0$, namely $g_1(x, Q_0^2) \propto x^{-\lambda}$ with $\lambda > 0$, then this behaviour remains unchanged by the evolution. But if one starts with a relatively flat distribution, for example one corresponding to the Regge behaviour (11.8.5), then as Q^2 grows the behaviour near $x = 0$ for $\Delta q_{NS}(x, Q^2)$, $\Delta \Sigma(x, Q^2)$ and $\Delta G(x, Q^2)$ tends to

$$(\xi \zeta)^{-1/4} \exp\left(2\gamma\sqrt{\xi \zeta} - \delta \zeta\right) \tag{11.8.6}$$

where

$$\xi = \ln \frac{x_0}{x} \qquad \zeta = \ln \left[\frac{\alpha_s(Q_0^2)}{\alpha_s(Q^2)} \right] \tag{11.8.7}$$

and x_0 is a small value of x below which the asymptotic treatment is valid. The coefficients γ and δ depend upon what density one is studying.

For Δq_{NS} one has

$$\begin{aligned} \gamma &= \gamma_{NS} = \left(\frac{8}{33 - 2N_f} \right)^{1/2} \\ \delta &= \delta_{NS} = \frac{4}{33 - 2N_f}. \end{aligned} \tag{11.8.8}$$

For both $\Delta \Sigma$ and ΔG ,

$$\begin{aligned} \gamma &= \gamma_+ = \left[\frac{8}{33 - 2N_f} \left(5 + 4\sqrt{1 - \frac{3}{32}N_f} \right) \right]^{1/2} \\ \delta &= \delta_+ = \frac{1}{2(33 - 2N_f)} \left[35 + 2N_f + 43 \left(\frac{1 - \frac{11}{86}N_f}{\sqrt{1 - \frac{3}{32}N_f}} \right) \right]. \end{aligned} \tag{11.8.9}$$

Moreover one finds the remarkable result that as $x \rightarrow 0$

$$\Delta\Sigma(x, Q^2) \rightarrow -2 \left(1 - \sqrt{1 - \frac{3}{32} N_f} \right) \Delta G(x, Q^2). \quad (11.8.10)$$

The implications of these results are fascinating.

- (1) All the polarized distributions grow faster than any power of $\ln x_0/x$, and the growth rate increases with Q^2 .
- (2) Since $\gamma_+ > \gamma_{NS}$, $\Delta\Sigma$ and ΔG dominate in magnitude over Δq_{NS} .
- (3) If $\Delta G(x, Q^2)$ is positive and reasonably large the negative contribution of $\Delta\Sigma$ will then make the sum $g_1^p + g_1^n$, and eventually each of g_1^p and g_1^n , *negative* at small enough x .

Interestingly, a similar analysis for the unpolarized case produces the required growth at small x to account for the HERA data mentioned above provided the starting value Q_0^2 is chosen small enough.

The situation is somewhat muddled by the work of Bartels, Ermolaev and Ryskin (1996a, b) and Manayenkov and Ryskin (1998), who sum 'double logarithmic' terms, of the form $(\alpha_s \ln^2 x)^n$, that are not included in the evolution equations, with the startling results that all the densities diverge as $x^{-\lambda}$, with $\lambda_{NS} \approx 0.5$ and $\lambda_S = \lambda_G \gtrsim 1$. The latter would imply that the first moment of $g_1^{p,n}$ diverges! It is difficult to believe that these results reflect the physical behaviour of the densities. It may be that such selective summations at fixed Q^2 are dangerous and that major cancellations can occur between different subsets of terms.

All the above results, based on a selective summation of terms in perturbation theory, disagree with Regge behaviour. Is this a genuine incompatibility or are the perturbative arguments unreliable at small enough x or small enough Q^2 ? And if the latter, at what scale should we expect to see Regge behaviour setting in? These are fascinating questions to which we have, as yet, no answer. A good discussion can be found in Altarelli, Ball, Forte and Ridolfi (1997). These authors also show that with a careful extrapolation to small x the Bjorken sum rule (11.6.19) is well satisfied by the present data.

As a final word on the subject of small- x behaviour, note that the *new*, 1996, SMC data on g_1^p (Fig. 11.12), combined with the new E154 data on g_1^n (Fig. 11.13), do suggest that $g_1^p + g_1^n$ might become negative at the smallest measured x -values!

There is a major experimental push towards smaller x . The results are awaited with great interest.

11.9 The general partonic structure of the nucleon

In Section 11.5 we saw how the parton model for DIS can be given a more fundamental field-theoretic formulation. Crucial to that derivation

was the separation of the physics into ‘hard’ and ‘soft’ parts, exemplified by $E^{\mu\nu}$ and Φ in (11.5.14) respectively. In Section 11.5 we took a specific form for $E^{\mu\nu}$ and concentrated upon its antisymmetric part under $\mu \leftrightarrow \nu$. But the steps taken are actually more general and would apply to any structure of the form

$$W = \int d^4k \text{Tr} [E(q, k)\Phi(P, \mathcal{S}; k)] \tag{11.9.1}$$

so long as $E(q, k)$ represents a hard process whose scale is set by q^2 and provided the approximation (11.5.28) is adequate.

The generalization of (11.5.31) and (11.5.32) is then

$$W = \text{Tr} [E(q, k)\hat{\Phi}(P, \mathcal{S}; n, x)] \tag{11.9.2}$$

where

$$\hat{\Phi}_{\alpha\beta} = \int \frac{d\lambda}{2\pi} e^{i\lambda x} \langle P, \mathcal{S} | \bar{\psi}_\beta(0) \psi_\alpha(\lambda n) | P, \mathcal{S} \rangle \tag{11.9.3}$$

and $k = xP$ in $E(q, k)$.¹

Being a 4×4 matrix in its Dirac labels, $\hat{\Phi}$ can be expanded in the form

$$\hat{\Phi} = sI + v_\mu \gamma^\mu - ip_{\mu\nu} \gamma_5 \sigma^{\mu\nu} + a_\mu \gamma^\mu \gamma_5 + ip \gamma_5. \tag{11.9.4}$$

The coefficients are given by traces of the form (Γ is some Dirac matrix)

$$\begin{aligned} \text{Tr} (\hat{\Phi}\Gamma) &= \int \frac{d\lambda}{2\pi} e^{i\lambda x} \langle P, \mathcal{S} | \bar{\psi}(0) \Gamma \psi(\lambda n) | P, \mathcal{S} \rangle \\ &\equiv \langle \Gamma \rangle \end{aligned} \tag{11.9.5}$$

for brevity. One has

$$\left. \begin{aligned} s &= \frac{1}{4} \langle I \rangle & p &= -\frac{1}{4} \langle i\gamma_5 \rangle \\ v_\mu &= \frac{1}{4} \langle \gamma_\mu \rangle & a_\mu &= \frac{1}{4} \langle \gamma_5 \gamma_\mu \rangle \\ p_{\mu\nu} &= \frac{1}{4} \langle i\gamma_5 \sigma_{\mu\nu} \rangle, \end{aligned} \right\} \tag{11.9.6}$$

these coefficients being scalar, pseudoscalar, vector, axial-vector and pseudo-tensor respectively. The coefficients can only be constructed from the large vector P_μ , the small vector n_μ and the axial vector \mathcal{S}_μ , and they can at most be linear in \mathcal{S}_μ . In addition the behaviour under hermitian conjugation, and the transformation laws for the fields under space inversion and time reversal (see Section 2.3), lead to the requirements

$$\hat{\Phi}^\dagger(P, \mathcal{S}; n) = \gamma_0 \hat{\Phi}(P, \mathcal{S}; n) \gamma_0 \tag{11.9.7}$$

$$\hat{\Phi}(P, \mathcal{S}; n) = \gamma_0 \hat{\Phi}(\tilde{P}, -\tilde{\mathcal{S}}; \tilde{n}) \gamma_0, \tag{11.9.8}$$

¹ In fact one can go beyond this approximation by making a Taylor expansion of $E(q, k)$ about the point $k = xP$. For details see Boer (1998).

where for any 4-vector $\tilde{V}^\mu = (V^0, -\mathbf{V})$, and

$$\hat{\Phi}(P, \mathcal{S}; n) = \gamma_5 C^{-1} \hat{\Phi}^T(P, -\mathcal{S}; n) C \gamma_5 \tag{11.9.9}$$

where T indicates the transpose and $C\gamma_\mu C^{-1} = -\gamma_\mu^T$.

It follows that $p = 0$ in (11.9.6). For the other coefficients, several terms are possible. They can be ordered into sets according to magnitude, the largest $O(|P|)$, the next $O(1)$ and so on. When linked to the hard process they give rise to terms of twist 2 and twist 3 respectively. ('Twist' was briefly mentioned in Section 11.7. For a more detailed explanation of this concept see, for example, Section 22.2 of Leader and Predazzi (1996)). For the purpose of this classification it is convenient to split the covariant spin vector into a longitudinal part $\mathcal{S}^\mu(\lambda)$ given by (11.5.35), and therefore 'large', and a transverse part

$$\mathcal{S}_T^\mu = (0, \mathcal{S}_T, 0) \tag{11.9.10}$$

of $O(1)$. We have

$$\begin{aligned} \hat{\Phi} = & \frac{P}{2} [f(x) - 2\lambda h_L(x)\gamma_5 + h_T(x)\gamma_5 \mathcal{S}_T] \\ & + \frac{M}{2} \{e(x)I + f_T(x)\gamma_5 \mathcal{S}_T + f_L(x)\lambda\gamma_5[P, \not{n}]\} \\ & + \dots \end{aligned} \tag{11.9.11}$$

There is confusion in the literature about the nomenclature of the coefficient functions in (11.9.11). We have essentially followed the logical notation in the ground-breaking paper of Ralston and Soper (1979) and in the later discussion of Cortes, Pire and Ralston (1992).

Unfortunately, an influential paper of Jaffe and Ji (1991) uses a quite different and potentially misleading notation. This labels some of the coefficient functions as g_1, g_2, g_3 , thereby confusing experimentally defined and measured quantities with approximate theoretical expressions for them. Up to an overall constant the relations between our coefficients and those of Jaffe and Ji are

$$\begin{aligned} h_L &= g_1^{JJ} & h_T &= h_1^{JJ} \\ f_T &= (g_1 + g_2)^{JJ} & f &= f_1^{JJ} \\ f_L &= (h_2 + \frac{1}{2}h_1)^{JJ} \end{aligned} \tag{11.9.12}$$

In principle a complete knowledge of the partonic structure of the nucleon would require a knowledge of all the coefficient functions in (11.9.11). It is hard to imagine that we will ever possess such detailed knowledge. In (11.9.11) the first three terms correspond to twist 2 and are the parton-model terms that would emerge if the quark fields ψ were treated as free fields. As explained in subsection 11.5.2 the term f_T , which

occurs in the expression (11.5.50) for $g_1 + g_2$, is not of twist 2 and does not emerge from the parton model.

All the coefficient functions in (11.9.11) are given by the nucleon matrix elements of bilocal light-cone operators. As such they depend not only upon x but, strictly speaking, upon the renormalization scale μ as well. Since this is, in principle, arbitrary, it is usual to choose it equal to the large scale in the reaction. For example, in DIS one chooses $\mu^2 = Q^2$.

In the shorthand notation of (11.9.5), with the spin state of the nucleon indicated by a subscript λ or \mathcal{S}_T for the longitudinal and transverse cases respectively, one has

$$\begin{aligned}
 h_L &= -\frac{1}{4\lambda} \langle \gamma_5 \not{n} \rangle_\lambda \\
 h_T &= -\frac{1}{2} \langle i\gamma_5 \sigma_{\mu\nu} \mathcal{S}_T^\mu n^\nu \rangle_{\mathcal{S}_T} \\
 f_T &= -\frac{1}{2M} \langle \gamma_5 \not{\mathcal{P}}_T \rangle_{\mathcal{S}_T} \\
 f_L &= \frac{1}{4M\lambda} \langle i\gamma_5 \sigma_{\mu\nu} n^\mu P^\nu \rangle_\lambda \\
 f &= \frac{1}{2} \langle \not{n} \rangle \\
 e &= \frac{1}{2M} \langle I \rangle.
 \end{aligned}
 \tag{11.9.13}$$

We mentioned in Section 11.5 that in the free-field or parton model

$$h_L(x) = \Delta q(x) = q_+(x) - q_-(x) \tag{11.9.14}$$

where \pm refers to the quark helicity inside a nucleon of helicity $+1/2$.

The function $h_T(x)$ is the analogue of this when the nucleon is polarized perpendicular to its momentum, and in the parton model

$$h_T(x) = \Delta_T q(x) = q_\uparrow(x) - q_\downarrow(x) \tag{11.9.15}$$

where $\uparrow\downarrow$ refer to the quark's transverse covariant spin vector being along or opposite to the spin of the transversely polarized nucleon.

Conventionally the transverse spin direction is chosen as the Y direction for a particle moving along the Z -axis. Then by (1.1.18)

$$\begin{aligned}
 |\mathbf{p}; \uparrow\rangle_y &= \frac{1}{\sqrt{2}} (|\mathbf{p}; 1/2\rangle + i|\mathbf{p}; -1/2\rangle) \\
 |\mathbf{p}; \downarrow\rangle_y &= \frac{1}{\sqrt{2}} (|\mathbf{p}; 1/2\rangle - i|\mathbf{p}; -1/2\rangle)
 \end{aligned}
 \tag{11.9.16}$$

where $\uparrow\downarrow$ means along or opposite to OY respectively.

Sometimes the X -direction is chosen, for which we have

$$\begin{aligned}
 |\mathbf{p}; \uparrow\rangle_x &= \frac{1}{\sqrt{2}} (|\mathbf{p}; 1/2\rangle + |\mathbf{p}; -1/2\rangle) \\
 |\mathbf{p}; \downarrow\rangle_x &= -\frac{1}{\sqrt{2}} (|\mathbf{p}; 1/2\rangle - |\mathbf{p}; -1/2\rangle).
 \end{aligned}
 \tag{11.9.17}$$

In DIS it is easy to see from (11.5.10) that the leading-order piece of $E(q, k)$ in (11.9.1), which describes the ‘hard’ process, always involves a product of an odd number of γ -matrices. Hence in the trace in (11.9.2) only that part of $\hat{\Phi}$ involving an odd number of γ -matrices will contribute, i.e. only the terms v_μ and a_μ in (11.9.4). The large term $h_T(x)$ is connected to the structure $\gamma_5\sigma_{\mu\nu}$, and hence does not appear in leading order in DIS. It can be measured in polarized Drell–Yan-type reactions, as is discussed in Section 12.4, and possibly also in single-spin asymmetries in semi-inclusive hadron–hadron reactions. (See, however, Section 13.4.)

It should be stressed that the functions $f(x), h_L(x)$ and $h_T(x)$ or, equivalently, $q(x), \Delta q(x)$ and $\Delta_T q(x)$ are on an equal footing and contain the most essential information about the internal partonic-spin structure of the nucleon. There is steady progress in the experimental determination of the $\Delta q(x)$ but, to date, we possess very little experimental information about the transverse densities $\Delta_T q(x)$. (See, however, Section 13.4.) Indeed, the only unambiguous information we have about $\Delta_T q(x)$ is the *Soffer bound* (Soffer, 1995):

$$|\Delta_T q(x)| \leq \frac{1}{2} [q(x) + \Delta q(x)]. \tag{11.9.18}$$

The importance of $\Delta_T q(x)$ was first stressed in a seminal paper by Ralston and Soper (1979), and the possibility of its measurement was discussed by Artru and Mekhfi (1990), by Jaffe and Ji (1991) and by Cortes, Pire and Ralston (1992). We shall discuss the phenomenological aspects of $\Delta_T q(x)$ in Section 12.4 and Chapter 13.

11.9.1 Evolution for $\Delta_T q(x, Q^2)$

The evolution equations for $\Delta_T q(x, Q^2)$ are similar in form to (11.7.2), but simpler since there is no gluon contribution. The evolution is thus analogous to that of a flavour non-singlet combination of polarized-quark densities.

The transverse-polarization splitting functions, in leading order, $\Delta_T P_{qq}^{(0)}$, were given by Artru and Mekhfi (1990). The next-to-leading-order result can be found in Vogelsang (1998).

At leading order the moments of the transversely polarized quark densities vary in a very simple way with Q^2 :

$$\Delta_T q^{(n)}(Q^2) = \left[\frac{\alpha_s(Q^2)}{\alpha_s(Q_0^2)} \right]^{-2\Delta_T P_{qq}^{(0)(n)}/\beta_0} \times \Delta_T q^{(n)}(Q_0^2) \quad n = 1, 2, \dots \tag{11.9.19}$$

where $\beta_0 = 11 - 2n_f/3$, n_f being the number of active flavours, and the moments $\Delta_T P_{qq}^{(0)(n)}$ of the splitting functions turn out to be negative for all n . It follows that all $\Delta_T q^{(n)}(Q^2)$ decrease as Q^2 increases. In general one cannot conclude that $\Delta_T q(x, Q^2)$ decreases in magnitude for all x as

Q^2 increases, but one can do so if $\Delta_T q(x, Q_0^2)$ is a monotonic function of x .

Strictly speaking, in NLO the combinations $\Delta_T q_{\pm} \equiv \Delta_T q \pm \Delta_T \bar{q}$ evolve with different splitting functions $\Delta_T P_{qq\pm}^{(1)}$, but it turns out that the difference between $\Delta_T P_{qq+}^{(1)}$ and $\Delta_T P_{qq-}^{(1)}$ is completely negligible. Hence, in practice $\Delta_T q$ and $\Delta_T \bar{q}$ can be considered to evolve with essentially the same splitting functions.

11.10 The future: neutrino beams?

There has been much discussion recently about the possibility of constructing a *muon collider* involving the collision of two circulating high energy muon beams. A prerequisite for this is a muon storage ring, which, it was suddenly realized, could provide a clean high energy neutrino beam of staggering intensity — 10^3 or 10^4 times more intense than present fluxes and well focussed. In fact the production via, say, $\mu^- \rightarrow e^- + \nu_{\mu} + \bar{\nu}_e$ actually produces, in a well-defined way, a mixture of neutrinos and antineutrinos. But it is a trivial matter to separate the neutrino from the antineutrino charged current reactions in the target by simply identifying the charge of the final state lepton. It is *not* necessary to separate high energy same-sign muons from electrons, which would have been a daunting task.

With this sort of flux it becomes possible to use targets of a few kilograms, rather than kilotonnes and, for the first time ever, to contemplate polarized target experiments with neutrino beams. This would indeed be a dramatic development. Flavour separation, i.e. the separate determination of the parton and antiparton densities of a given flavour, has only been possible for the unpolarized case because of the ability to combine data from neutral current and charged current reactions. With this exciting prospect in view we shall here present a brief outline of how and what could be measured for neutrino and antineutrino *CC* reactions.

Because of the parity-violating electroweak coupling one no longer has the correspondence that the symmetric part $W_{\mu\nu}^{(S)}$ in (11.3.9) is spin independent and the antisymmetric part $W_{\mu\nu}^{(A)}$ in (11.3.10) is spin dependent. Now the spin-dependent part of $W_{\mu\nu}$ is a superposition of symmetric and antisymmetric pieces and involves five independent structure functions $g_j(x, Q^2)$, which, in the absence of strong interactions, would obey Bjorken scaling, i.e. would be independent of Q^2 . There is a plethora of different definitions of the g_j in the literature. We shall follow the definitions used in the recent very important paper of Blümlein and Kochelev (1997).¹

¹ These g_j are related to the g_j^{AEL} used in the review article by Anselmino, Efremov and Leader (1995) via $g_{1,2} = g_{1,2}^{\text{AEL}}$; $g_3 = -g_3^{\text{AEL}}$; $g_4 = g_4^{\text{AEL}} - g_3^{\text{AEL}}$; $g_5 = -g_5^{\text{AEL}}$.

Then, using the same kinematic variables as in Section 11.3 and defining

$$\hat{P}_\mu = P_\mu - \frac{P \cdot q}{q^2} q_\mu \tag{11.10.1}$$

$$\hat{\mathcal{S}}_\mu = \mathcal{S}_\mu - \frac{\mathcal{S} \cdot q}{q^2} q_\mu \tag{11.10.2}$$

one has for the spin-dependent part

$$\begin{aligned} \frac{1}{2M} W_{\mu\nu} = & \frac{\epsilon_{\mu\nu\alpha\beta} q^\alpha}{P \cdot q} \left[\mathcal{S}^\beta g_1 + \frac{(P \cdot q \mathcal{S}^\beta - \mathcal{S} \cdot q P^\beta)}{P \cdot q} g_2 \right] \\ & + \left(\frac{\hat{P}_\mu \hat{\mathcal{S}}_\nu + \hat{\mathcal{S}}_\mu \hat{P}_\nu}{2} - \mathcal{S} \cdot q \frac{\hat{P}_\mu \hat{P}_\nu}{P \cdot q} \right) g_3 \\ & + \mathcal{S} \cdot q \left[\frac{\hat{P}_\mu \hat{P}_\nu}{P \cdot q} g_4 + \left(-g_{\mu\nu} + \frac{q_\mu q_\nu}{q^2} \right) g_5 \right] \end{aligned} \tag{11.10.3}$$

where we have suppressed the neutrino labels ν and $\bar{\nu}$ that should be attached to $W_{\mu\nu}$ and the g_j .

The differential cross-section differences for the longitudinally and transversely polarized target cases are related to the g_j as follows.

For ν or $\bar{\nu}$ beams on a target polarized longitudinally, along (\Rightarrow) or opposite (\Leftarrow) to the initial lepton beam direction,

$$\begin{aligned} \frac{d^2\sigma^{\nu,\bar{\nu}}(\Leftarrow)}{dxdy} - \frac{d^2\sigma^{\nu,\bar{\nu}}(\Rightarrow)}{dxdy} = & 32\pi s \frac{\alpha^2}{Q^4} \eta_W \\ & \times \left[\pm \left(2 - y - 2xy \frac{M^2}{s} \right) yxg_1 \mp \frac{4M^2}{s} yx^2g_2 \right. \\ & + \frac{2M^2}{s} \left(1 - y - xy \frac{M^2}{s} \right) xg_3 \\ & - \left(1 + 2x \frac{M^2}{s} \right) \left(1 - y - xy \frac{M^2}{s} \right) g_4 \\ & \left. + \left(1 + 2x \frac{M^2}{s} \right) y^2 xg_5 \right] \end{aligned} \tag{11.10.4}$$

where \sqrt{s} is the CM energy of the lepton–nucleon collision ($s \approx 2ME$), and

$$\eta_W = \frac{1}{2} \left(\frac{GM_W^2}{4\pi\alpha} \frac{Q^2}{Q^2 + M_W^2} \right)^2 \tag{11.10.5}$$

In (11.10.4) one must use $g_j^{W^-}$ for neutrino beams, and $g_j^{W^+}$ for antineutrino beams.

It is perfectly reasonable to neglect terms of order M^2/s , so that one obtains the simpler result

$$\frac{d^2\sigma^{v,\bar{v}}(\Leftarrow)}{dxdy} - \frac{d^2\sigma^{v,\bar{v}}(\Rightarrow)}{dxdy} \approx 32\pi s \frac{\alpha^2}{Q^4} \eta_W \left[\pm(2-y)yxg_1^{W^\mp} - (1-y)g_4^{W^\mp} + y^2xg_5^{W^\mp} \right]. \quad (11.10.6)$$

For a transversely polarized target (\uparrow or \downarrow), with ϕ , the azimuthal angle of the final state lepton, measured with respect to the plane formed by the initial lepton momentum and the nucleon spin direction \uparrow (see Fig. 11.17), one has

$$\begin{aligned} \frac{d^3\sigma^{v,\bar{v}}(\uparrow)}{dxdyd\phi} - \frac{d^3\sigma^{v,\bar{v}}(\downarrow)}{dxdyd\phi} &= 16M\sqrt{s} \frac{\alpha^2}{Q^4} \eta_W \cos\phi \left[xy \left(1 - y - xy \frac{M^2}{s} \right) \right] \\ &\times \left\{ \pm 2yxg_1 \pm 4g_2 - \frac{1}{y} \left(2 - y - 2xy \frac{M^2}{s} \right) g_3 \right. \\ &\quad \left. + \frac{2}{y} \left(1 - y - xy \frac{M^2}{s} \right) g_4 + 2y^2xg_5 \right\}. \end{aligned} \quad (11.10.7)$$

Just as for the case of g_2 in electromagnetic neutral current reactions, (Section 11.4 and subsection 11.5.2) the structure functions g_2^W and g_3^W cannot be calculated in the simple parton model. For the other g_j^W one finds

$$g_1^{W^-} = \Delta u + \Delta c + \Delta \bar{d} + \Delta \bar{s} \quad (11.10.8)$$

$$g_5^{W^-} = \Delta \bar{d} + \Delta \bar{s} - \Delta u - \Delta c \quad (11.10.9)$$

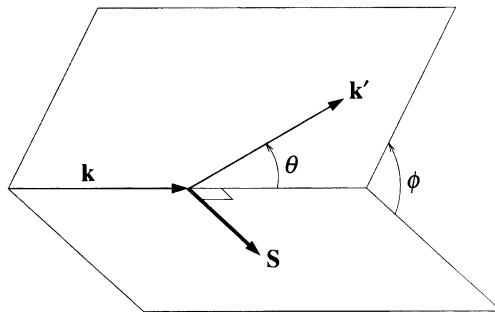


Fig. 11.17. Definition of azimuthal angle ϕ for transverse nucleon polarization. The bold horizontal arrow gives the nucleon spin direction.

and (Dicus, 1972)

$$g_4^{W^\mp} = 2xg_5^{W^\mp} \tag{11.10.10}$$

and

$$g_1^{W^+} = \Delta d + \Delta s + \Delta \bar{u} + \Delta \bar{c} \tag{11.10.11}$$

$$g_5^{W^+} = \Delta d + \Delta s - \Delta \bar{u} - \Delta \bar{c}. \tag{11.10.12}$$

In all these it is probably safe to take $\Delta c = \Delta \bar{c} = 0$.

At the parton level, (11.10.6) simplifies to

$$\begin{aligned} & \frac{d^2\sigma^{v,\bar{v}}(\Leftarrow)}{dxdy} - \frac{d^2\sigma^{v,\bar{v}}(\Rightarrow)}{dxdy} \\ & \approx 32\pi s \frac{\alpha^2}{Q^4} \eta_W \left\{ \pm(2-y)yxg_1^{W^\mp} + [y^2 - 2(1-y)]xg_5^{W^\mp} \right\} \end{aligned} \tag{11.10.13}$$

so that it might not be too difficult to determine g_1 and g_5 separately.

In that case one would be able to make a direct measurement of the flavour-singlet combination $\Delta\Sigma$, which plays such a crucial rôle in the ‘spin crisis’ (Section 11.2 and subsection 11.6.1). For one has

$$g_1^{W^-} + g_1^{W^+} = \Delta u + \Delta \bar{u} + \Delta d + \Delta \bar{d} + \Delta s + \Delta \bar{s} + \Delta c + \Delta \bar{c}. \tag{11.10.14}$$

The advent of neutrino-induced polarized DIS would open up an extremely rich and valuable source of information on the internal structure of the nucleon. It is to be hoped that such experiments do not lie too far into the future.